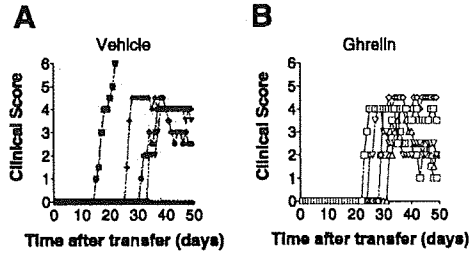

FIGURE 4. Effects of ghrelin treatment on the induction of encephalitogenic T cells. MOG_{35-55}-sensitized lymphoid cells were derived from MOG_{35-55}-immunized and (*A*) saline- or (*B*) ghrelin-treated mice (n = 15/group). The cells were stimulated with MOG_{35-55} and $CD4^+$ T cells were separated 3 days later for passive transfer of EAE into naive mice (n = 5/group). Data represent individual EAE score for each mouse.

inhibit induction of MOG_{35-55}-reactive T cells, but would prohibit the ability to cause EAE in vivo. In postulating that this could happen, $CD4^+$ T cells from ghrelin-treated donors should be less encephalitogenic than those from saline-treated mice. The results showed that transfer of activated $CD4^+$ T cells either derived from saline- or ghrelin-treated donors induced passive EAE in the recipients, showing approximately the same clinical course and severity (Fig. 4). Thus, it can be concluded that ghrelin treatment does not affect the induction of encephalitogenic MOG_{35-55}-reactive $CD4^+$ T cells.

Ghrelin decreases mRNA levels of proinflammatory cytokines in the CNS

After demonstrating that ghrelin does not suppress the infiltration of inflammatory cells in the spinal cord, we wondered whether the cytokine milieu in the ghrelin-treated mice could be significantly altered. To answer the question, we analyzed the mRNA levels of pro- and antiinflammatory cytokines (IFN-γ, TNF-α, IL-1β, IL-6, IL-4, IL-10, and TGF-β) in the spinal cord, spleen, LN, and thymus of ghrelin- and saline-treated mice at the peak of disease (day 17) by using quantitative PCR. Although ghrelin treatment had no effect on the mRNA levels of IL-4, IL-10, and IFN-γ in the spinal cord, spleen, LN, and thymus (data not shown), we found significantly reduced levels of TNF-α ($p < 0.0015$), IL-1β ($p < 0.025$), and IL-6 ($p < 0.025$) in the spinal cord of ghrelin-treated mice, compared with saline-treated ones (Fig. 5*A*). In contrast, the level of TGF-β showed a trend for slight elevation in the spinal cord. We also found a diminished level of TNF-α mRNA ($p < 0.0001$) in the spleen of ghrelin-treated mice (Fig. 5*B*), whereas we saw no significant change in any of the cytokines that we measured in LN or thymus of ghrelin-treated mice (Fig. 5, *C* and *D*). Because TNF-α, IL-1β, and IL-6 mRNAs were selectively down-regulated in the spinal cord, we suspected that monocytes could be potential target cells in the ghrelin-mediated EAE suppression. This idea was consistent with the fact that ghrelin treatment did not inhibit the induction of MOG_{35-55}-reactive T cells.

Ghrelin suppresses the proinflammatory cytokine production of LPS-stimulated monocytes

To verify the postulate that in vivo treatment with ghrelin may ameliorate EAE by targeting monocytes, we examined in vitro effects of ghrelin on the monocytic cell line RAW 264.7 that robustly produce proinflammatory cytokines when stimulated with LPS. The RAW 264.7 line cells were first exposed to various doses of ghrelin for 1 h and then stimulated with LPS. We harvested the supernatant 2 h later and measured the levels of TNF-α and IL-6 by ELISA. The results revealed that prior exposure to ghrelin

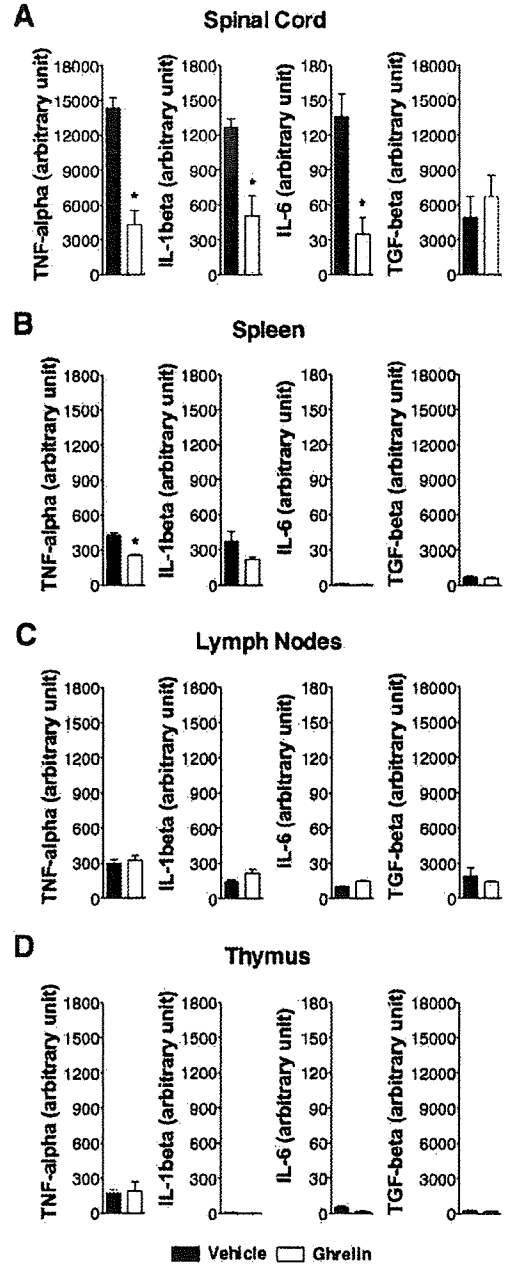

FIGURE 5. Proinflammatory cytokine mRNA expression during EAE in ghrelin-treated mice. Quantitative mRNA expression of proinflammatory cytokines in the spinal cord of MOG_{35-55}-immunized mice subjected to ghrelin or saline treatment on day 17 postimmunization (n = 5/group). Total mRNA was extracted from (*A*) spinal cord, (*B*) spleen, (*C*) LN, and (*D*) thymus. The TNF-α, IL-1β, IL-6, and TGF-β mRNA expression was measured by real-time PCR. Data are presented as relative amount of transcript normalized to HPRT. Data represent mean ± SEM. *, Significant differences between the groups ($p < 0.025$; two-way ANOVA).

would significantly suppress the production of TNF-α ($p < 0.02$) and IL-6 ($p < 0.05$) by LPS-stimulated RAW 264.7 cells in a dose-dependent manner (Fig. 6). The inhibitory effect of ghrelin was very potent, as in addition to the effects on LPS-stimulated monocytes, even the basal production of TNF-α ($p < 0.008$) and IL-6 ($p < 0.03$) was significantly reduced by in vitro ghrelin treatment. Given that in vivo treatment with ghrelin could suppress the

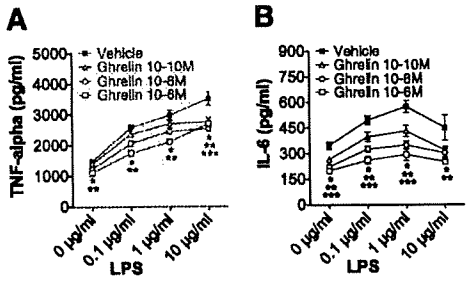

FIGURE 6. Effect of ghrelin on the proinflammatory cytokine production of LPS-stimulated monocytes. The monocytes were treated with various concentrations of ghrelin (10^{-6} M, 10^{-8} M, 10^{-10} M) 1 h before stimulation with 0.1, 1.0, and 10 μg/ml LPS. The (*A*) TNF-α and (*B*) IL-6 production was measured 2 h after LPS stimulation by sandwich ELISA. Data represent mean ± SEM of duplicate samples from one out of three independent experiments. Significant differences at 10^{-6}, 10^{-8}, and 10^{-10} M ($p < 0.05$; two-way ANOVA) are depicted as *, **, and ***, respectively.

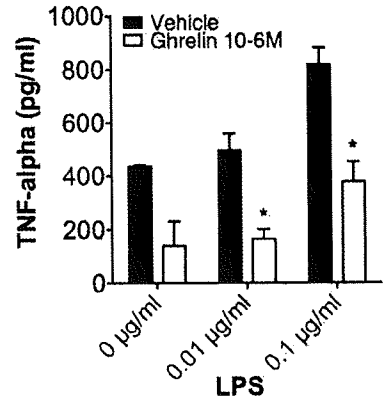

FIGURE 8. Effect of ghrelin on the proinflammatory cytokine production of LPS-stimulated microglia. The microglia cells were treated with ghrelin (10^{-6} M) overnight and later stimulated with 0.01 and 0.1 μg/ml LPS. Five hours after stimulation, the TNF-α production was measured using ELISA. Data represent mean ± SEM of duplicate samples from one out of two independent experiments. *, Significant differences between the groups ($p < 0.05$; two-way ANOVA).

development of EAE without altering histological EAE or T cell-derived cytokine balance, the ghrelin-mediated suppression of monocyte-produced TNF-α and IL-6 would strongly support the postulate that monocytes are the main target cells in ghrelin-mediated suppression of EAE.

Ghrelin inhibits the expression of proinflammatory cytokines in microglia

The proinflammatory cytokines are known to be produced not only by CNS-infiltrating macrophages but also by T cells and microglia in the course of EAE. To investigate which cells are important in the ghrelin-mediated suppression of EAE, we first examined the expression of proinflammatory cytokines in macrophages. Unexpectedly, the mRNA of IL-1β, IL-6, and TNF-α did not alter in CNS-infiltrating macrophages of ghrelin-treated mice compared with the control mice (Fig. 7*A*). We next examined the expression of these cytokines in other cell types also known as a source of inflammatory cytokines and found reduced expression of these cytokines in microglia (Fig. 7*B*). Additionally, the expression of inflammatory cytokines was decreased in CNS-infiltrating T cells (Fig. 7*C*). Hence, these results suggest that microglia might play a crucial role in ghrelin-mediated inhibition of EAE.

Ghrelin inhibits the proinflammatory cytokine production of LPS-stimulated microglia

We next examined the effect of ghrelin on microglia. To test whether ghrelin directly affects microglia, we isolated mononuclear cells from the brains of untreated mice. In untreated non-EAE mice, most (~77%) of the brain mononuclear cells were CD11b$^+$ cells, and the majority of CD11b$^+$ cells (~95%) were considered as CD45^{low} microglia cells. Among these mononuclear cells, CD19$^+$ B cells were <0.1% and CD3$^+$CD45$^+$ T cells were 1–1.5%. We cultured the isolated mononuclear cells in the presence of ghrelin overnight and stimulated them with LPS in different doses for 5 h. The TNF-α levels in the culture supernatant were measured by using ELISA. In the presence of ghrelin, the TNF-α levels were significantly reduced (Fig. 8). These results suggest that ghrelin directly affects microglia by reducing the production of inflammatory cytokines.

Discussion

Starvation is known to have immunosuppressive effects (24–26). Although little was known about the mechanistic link between starvation and immunity, recent studies have shed light on the immunomodulatory potency of a range of feeding regulatory hormones such as leptin and NPY. For example, serum leptin is decreased after acute starvation in parallel with immunosuppression or Th2 bias, whereas exogenous leptin would correct the altered Th1/Th2 balance toward Th1 (27, 28). In contrast, NPY is increased after starvation. Exogenous NPY would shift the Th1/Th2 balance toward Th2 and can ameliorate the severity of EAE (29). Interestingly, both peptide hormones are linked to ghrelin in an endocrine feedback system (30). Ghrelin itself is increased after

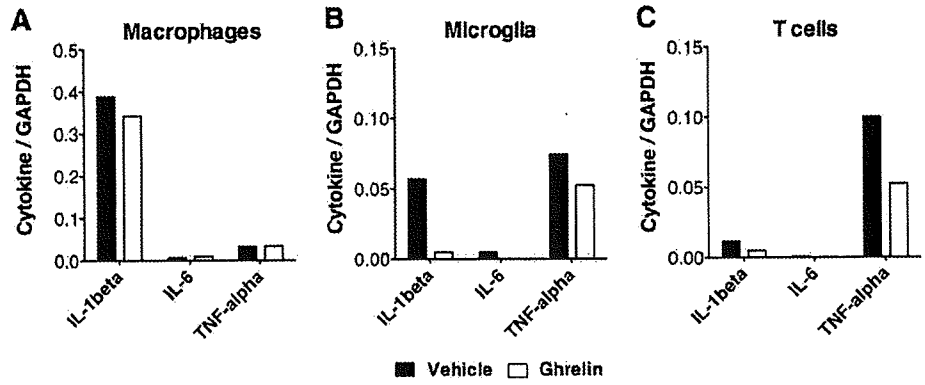

FIGURE 7. Effect of ghrelin on proinflammatory cytokine mRNA expression in infiltrating cells and microglia. Total mRNA was extracted from (*A*) macrophages, (*B*) microglia, and (*C*) T cells obtained on day 20 postimmunization from the spinal cords of MOG_{35-55}-immunized mice treated with ghrelin or saline. The IL-1β, IL-6, and TNF-α mRNA expression levels were measured by real-time PCR. Data are presented as relative amount of transcript normalized to the housekeeping gene GAPDH.

starvation, and it can potently stimulate the release of NPY in the CNS (12). Moreover, ghrelin shows antagonistic effects against leptin (31). Although the available data on the action of ghrelin on leptin or NPY may not be extrapolated to speculate about its role in the immune system, we decided to explore whether ghrelin may exhibit beneficial effects in the modulation of EAE. Furthermore, ghrelin was reported to have protective effects on endotoxic shock in rats (32). Additionally, the wide range of GHS-R expression within the immune cells strongly suggested the immunomodulatory potential of ghrelin (6). Considering its endocrine interactions, ghrelin becomes an interesting candidate for the in vivo modulation of EAE.

To evaluate the effects of ghrelin on the immune system in vivo, we used the representative EAE model induced with MOG_{35-55} in B6 mice. Subcutaneous injections of ghrelin significantly suppressed EAE severity, especially after the peak of disease, while the EAE onset occurred almost similarly in both ghrelin- and sham-treated mice. Priming phase treatment (days 1–10) as well as effector phase treatment (days 11–20) also showed disease-suppressing effects, suggesting a modulatory role of ghrelin during all phases of disease. The unacylated ghrelin form, des-acyl ghrelin, failed to suppress EAE, demonstrating that the disease suppression was mediated by the GHS-R.

The histological findings at day 17 were similar in all animals regardless of the applied treatment. The inflammatory cell infiltration and demyelination occurred in both groups, suggesting a ghrelin effect independent of cell trafficking at the peak of disease. Moreover, we found by FACS analysis that the number of mononuclear cells isolated from the spinal cord and their composition did not significantly alter among ghrelin- and sham-treated mice at the same time point. Our data showed no statistically significant changes in the examined cell subsets, which supported the histological findings of unaffected immune cell traffic to the CNS. This discrepancy between analogous inflammatory status in the spinal cord on the one hand and less severe disease on the other hand in ghrelin-treated mice was remarkable, suggesting cytokine regulation as the possible mechanism of EAE suppression.

Leptin and NPY both influence the Th1/Th2 balance in opposing directions (27–29). Since ghrelin is the most potent NPY-releasing hormone and NPY suppresses EAE by a Th2 bias (29), we examined whether ghrelin affects the Th1/Th2 balance similar to NPY and if its potential mechanism of EAE suppression is primarily mediated on immune cells or secondarily through NPY release. To investigate the effect of ghrelin on the cytokine balance, we measured the cytokine responses of MOG_{35-55}-primed T cells from mice treated with ghrelin or saline. The evaluated IFN-γ, IL-17, and IL-4 levels as well as the proliferative response did not significantly alter between ghrelin- and sham-treated mice. Underlying these observations, we conclude that the suppression of EAE mediated by ghrelin does not affect the T cell-derived cytokine balance. To further address whether ghrelin acts via the NPY pathway, we determined the encephalitogenic potential of $CD4^+$ T cells from ghrelin-treated mice to cause passive EAE in syngeneic recipients. We treated donor animals with ghrelin or saline for 10 days after priming with MOG_{35-55}, and lymphoid cells from the mice were stimulated with MOG_{35-55}. Three days later, $CD4^+$ T cell blasts were isolated and transferred to naive mice. The $CD4^+$ T cells from ghrelin-treated mice did not differ from those from saline-treated mice in the ability to mediate passive EAE, indicating that ghrelin does not primarily affect induction of encephalitogenic $CD4^+$ T cells in vivo. While NPY attenuates EAE by a Th2 bias of encephalitogenic $CD4^+$ T cells (29), our findings likely suggest that ghrelin interacts independently of NPY in the amelioration of EAE.

To further clarify the mechanism of ghrelin-mediated EAE suppression, we examined the mRNA levels of several cytokines of ghrelin- and sham-treated mice at the peak of disease. Our data demonstrate significantly reduced levels of the proinflammatory cytokines TNF-α, IL-1β, and IL-6 in the spinal cord and lower levels of TNF-α in the spleen of ghrelin-treated mice. In contrast, the level of TGF-β showed a trend for slight elevation in the spinal cord. The importance of TNF-α for initiating and sustaining inflammation is well described, as well as its essential role in the development of acute EAE (33, 34). The proinflammatory role of IL-1β and IL-6 in the immunopathology of EAE is also generally accepted (35–38). Thus, the inhibition of TNF-α, IL-1β, and IL-6 must be considered as an important mechanism in the ghrelin-mediated EAE suppression.

Given the selective down-modulation of the proinflammatory cytokines, we suspected that monocytes could be potential target cells in the ghrelin-mediated EAE suppression. However, the analysis of infiltrating cells and residential microglia revealed that the suppression of proinflammatory cytokines was prominently led by microglia. A decreased expression of these cytokines was also observed in infiltrating T cells. Considering that the transfer of T cells obtained from ghrelin-treated mice induced a similar disease course compared with control mice, the reduction of proinflammatory cytokines in microglia might be important in the ghrelin-mediated suppression of EAE.

In conclusion, the present study demonstrates for the first time to our knowledge that the gastric hormone ghrelin suppresses actively induced EAE by inhibiting production of the proinflammatory cytokines TNF-α, IL-1β, and IL-6 with microglia as the main target cells. These findings support an antiinflammatory property of ghrelin, shedding light on its role in immune-endocrine interactions. Consequently, we speculate that ghrelin may serve as an antiinflammatory drug to control human CNS pathology involving the production of proinflammatory cytokines.

Disclosures

The authors have no financial conflicts of interest.

References

1. Deghenghi, R., M. M. Cananzi, A. Torsello, C. Battisti, E. E. Muller, and V. Locatelli. 1994. GH-releasing activity of Hexarelin, a new growth hormone releasing peptide, in infant and adult rats. *Life Sci.* 54: 1321–1328.
2. Howard, A. D., S. D. Feighner, D. F. Cully, J. P. Arena, P. A. Liberator, C. I. Rosenblum, M. Hamelin, D. L. Hreniuk, O. C. Palyha, J. Anderson, et al. 1996. A receptor in pituitary and hypothalamus that functions in growth hormone release. *Science* 273: 974–977.
3. Smith, R. G., K. Cheng, W. R. Schoen, S. S. Pong, G. Hickey, T. Jacks, B. Butler, W. W. Chan, L. Y. Chaung, F. Judith, et al. 1993. A nonpeptidyl growth hormone secretagogue. *Science* 260: 1640–1643.
4. Kojima, M., H. Hosoda, Y. Date, M. Nakazato, H. Matsuo, and K. Kangawa. 1999. Ghrelin is a growth-hormone-releasing acylated peptide from stomach. *Nature* 402: 656–660.
5. Date, Y., M. Kojima, H. Hosoda, A. Sawaguchi, M. S. Mondal, T. Suganuma, S. Matsukura, K. Kangawa, and M. Nakazato. 2000. Ghrelin, a novel growth hormone-releasing acylated peptide, is synthesized in a distinct endocrine cell type in the gastrointestinal tracts of rats and humans. *Endocrinology* 141: 4255–4261.
6. Hattori, N., T. Saito, T. Yagyu, B. H. Jiang, K. Kitagawa, and C. Inagaki. 2001. GH, GH receptor, GH secretagogue receptor, and ghrelin expression in human T cells, B cells, and neutrophils. *J. Clin. Endocrinol. Metab.* 86: 4284–4291.
7. Hosoda, H., M. Kojima, H. Matsuo, and K. Kangawa. 2000. Ghrelin and des-acyl ghrelin: two major forms of rat ghrelin peptide in gastrointestinal tissue. *Biochem. Biophys. Res. Commun.* 279: 909–913.
8. Nakazato, M., N. Murakami, Y. Date, M. Kojima, H. Matsuo, K. Kangawa, and S. Matsukura. 2001. A role for ghrelin in the central regulation of feeding. *Nature* 409: 194–198.
9. Tschop, M., D. L. Smiley, and M. L. Heiman. 2000. Ghrelin induces adiposity in rodents. *Nature* 407: 908–913.
10. Muccioli, G., M. Tschop, M. Papotti, R. Deghenghi, M. Heiman, and E. Ghigo. 2002. Neuroendocrine and peripheral activities of ghrelin: implications in metabolism and obesity. *Eur. J. Pharmacol.* 440: 235–254.

11. Nagaya, N., T. Itoh, S. Murakami, H. Oya, M. Uematsu, K. Miyatake, and K. Kangawa. 2005. Treatment of cachexia with ghrelin in patients with COPD. *Chest* 128: 1187–1193.
12. Cowley, M. A., R. G. Smith, S. Diano, M. Tschop, N. Pronchuk, K. L. Grove, C. J. Strasburger, M. Bidlingmaier, M. Esterman, M. L. Heiman, et al. 2003. The distribution and mechanism of action of ghrelin in the CNS demonstrates a novel hypothalamic circuit regulating energy homeostasis. *Neuron* 37: 649–661.
13. Shintani, M., Y. Ogawa, K. Ebihara, M. Aizawa-Abe, F. Miyanaga, K. Takaya, T. Hayashi, G. Inoue, K. Hosoda, M. Kojima, et al. 2001. Ghrelin, an endogenous growth hormone secretagogue, is a novel orexigenic peptide that antagonizes leptin action through the activation of hypothalamic neuropeptide Y/Y1 receptor pathway. *Diabetes* 50: 227–232.
14. Dixit, V. D., E. M. Schaffer, R. S. Pyle, G. D. Collins, S. K. Sakthivel, R. Palaniappan, J. W. Lillard, Jr., and D. D. Taub. 2004. Ghrelin inhibits leptin- and activation-induced proinflammatory cytokine expression by human monocytes and T cells. *J. Clin. Invest.* 114: 57–66.
15. Wassem, T., M. Duxbury, H. Ito, S. W. Ashley, and M. K. Robinson. 2008. Exogeneous ghrelin modulates release of pro- and anti-inflammatory cytokines in LPS-stimulated macrophages through distinct signaling pathways. *Surgery* 143: 334–342.
16. Chorny, A., P. Anderson, E. Gonzalez-Rey, and M. Delgado. 2008. Ghrelin protects against experimental sepsis by inhibiting high-mobility group box 1 release and by killing bacteria. *J. Immunol.* 180: 8369–8377.
17. Gonzalez-rey, E., A. Chorny, and M. Delgado. 2006. Therapeutic action of ghrelin in a mouse model of colitis. *Gastroenterology* 130: 1707–1720.
18. Granado, M., T., Priego, A. I., Martin, A., Villanua, and A. Lopez-Caldron. 2005. Anti-inflammatory effect of the ghrelin agonist growth hormone-releasing peptide-2 (GHRP-2) in arthritic rats. *Am. J. Physiol.* 288: E486–E492.
19. Li, W. G., D. Gavrila, X. Liu, L. Wang, S. Gunnlaugsson, L. L. Stoll, M. L. McCormick, C. D. Sigmund, C. Tang, and N. L. Weintraub. 2004. Ghrelin inhibits proinflammatory responses and nuclear factor-κB activation in human endothelial cells. *Circulation* 109: 2221–2226.
20. Wu, R., W. Dong, X. Cui, M. Zhou, H. H. Simms, T. S. Ravikumar, and P. Wang. 2007. Ghrelin down-regulates proinflammatory cytokines in sepsis through activation of the vagus nerve. *Ann. Surg.* 245: 480–486.
21. Mendel, I., N. Kerlero de Rosbo, and A. Ben-Nun. 1995. A myelin oligodendrocyte glycoprotein peptide induces typical chronic experimental autoimmune encephalomyelitis in H-2b mice: fine specificity and T cell receptor Vβ expression of encephalitogenic T cells. *Eur. J. Immunol.* 25: 1951–1959.
22. Zhang, B., T. Yamamura, T. Kondo, M. Fujiwara, and T. Tabira. 1997. Regulation of experimental autoimmune encephalomyelitis by natural killer (NK) cells. *J. Exp. Med.* 186: 1677–1687.
23. Miyamoto, K., S. Miyake, M. Mizuno, N. Oka, S. Kusunoki, and T. Yamamura. 2006. Selective COX-2 inhibitor celecoxib prevents experimental autoimmune encephalomyelitis through COX-2-independent pathway. *Brain* 129: 1984–1992.
24. Chan, J. L., G. Matarese, G. K. Shetty, P. Raciti, I. Kelesidis, D. Aufiero, V. De Rosa, F. Perna, S. Fontana, and C. S. Mantzoros. 2006. Differential regulation of metabolic, neuroendocrine, and immune function by leptin in humans. *Proc. Natl. Acad. Sci. USA* 103: 8481–8486.
25. Kuchroo, V. K., and L. B. Nicholson. 2003. Immunology: fast and feel good? *Nature* 422: 27–28.
26. Wing, E. J., D. M. Magee, and L. K. Barczynski. 1988. Acute starvation in mice reduces the number of T cells and suppresses the development of T-cell-mediated immunity. *Immunology* 63: 677–682.
27. Lord, G. M., G. Matarese, J. K. Howard, R. J. Baker, S. R. Bloom, and R. I. Lechler. 1998. Leptin modulates the T-cell immune response and reverses starvation-induced immunosuppression. *Nature* 394: 897–901.
28. Sanna, V., A. Di Giacomo, A. La Cava, R. I. Lechler, S. Fontana, S. Zappacosta, and G. Matarese. 2003. Leptin surge precedes onset of autoimmune encephalomyelitis and correlates with development of pathogenic T cell responses. *J. Clin. Invest.* 111: 241–250.
29. Bedoui, S., S. Miyake, Y. Lin, K. Miyamoto, S. Oki, N. Kawamura, A. Beck-Sickinger, S. von Horsten, and T. Yamamura. 2003. Neuropeptide Y (NPY) suppresses experimental autoimmune encephalomyelitis: NPY1 receptor-specific inhibition of autoreactive Th1 responses in vivo. *J. Immunol.* 171: 3451–3458.
30. Kalra, S. P., and P. S. Kalra. 2003. Neuropeptide Y: a physiological orexigen modulated by the feedback action of ghrelin and leptin. *Endocrine* 22: 49–56.
31. Kalra, S. P., N. Ueno, and P. S. Kalra. 2005. Stimulation of appetite by ghrelin is regulated by leptin restraint: peripheral and central sites of action. *J. Nutr.* 135: 1331–1335.
32. Chang, L., J. Zhao, J. Yang, Z. Zhang, J. Du, and C. Tang. 2003. Therapeutic effects of ghrelin on endotoxic shock in rats. *Eur. J. Pharmacol.* 473: 171–176.
33. Glabinski, A. R., B. Bielecki, J. A. Kawczak, V. K. Tuohy, K. Selmaj, and R. M. Ransohoff. 2004. Treatment with soluble tumor necrosis factor receptor (sTNFR):Fc/p80 fusion protein ameliorates relapsing-remitting experimental autoimmune encephalomyelitis and decreases chemokine expression. *Autoimmunity* 37: 465–471.
34. Xanthoulea, S., M. Pasparakis, S. Kousteni, C. Brakebusch, D. Wallach, J. Bauer, H. Lassmann, and G. Kollias. 2004. Tumor necrosis factor (TNF) receptor shedding controls thresholds of innate immune activation that balance opposing TNF functions in infectious and inflammatory diseases. *J. Exp. Med.* 200: 367–376.
35. Furlan, R., A. Bergami, E. Brambilla, E. Butti, M. G. De Simoni, M. Campagnoli, P. Marconi, G. Comi, and G. Martino. 2007. HSV-1-mediated IL-1 receptor antagonist gene therapy ameliorates MOG_{35-55}-induced experimental autoimmune encephalomyelitis in C57BL/6 mice. *Gene Ther.* 14: 93–98.
36. Okuda, Y., S. Sakoda, H. Fujimura, Y. Saeki, T. Kishimoto, and T. Yanagihara. 1999. IL-6 plays a crucial role in the induction phase of myelin oligodendrocyte glucoprotein 35–55 induced experimental autoimmune encephalomyelitis. *J. Neuroimmunol.* 101: 188–196.
37. Okuda, Y., S. Sakoda, Y. Saeki, T. Kishimoto, and T. Yanagihara. 2000. Enhancement of Th2 response in IL-6-deficient mice immunized with myelin oligodendrocyte glycoprotein. *J. Neuroimmunol.* 105: 120–123.
38. Sutton, C., C. Brereton, B. Keogh, K. H. Mills, and E. C. Lavelle. 2006. A crucial role for interleukin (IL)-1 in the induction of IL-17-producing T cells that mediate autoimmune encephalomyelitis. *J. Exp. Med.* 203: 1685–1691.

The American Journal of Pathology, Vol. 175, No. 3, September 2009

DOI: 10.2353/ajpath.2009.090265

Immunopathology and Infectious Diseases

Carcinoembryonic Antigen-Related Cell Adhesion Molecule 1 Modulates Experimental Autoimmune Encephalomyelitis via an iNKT Cell-Dependent Mechanism

Mayumi Fujita,* Takao Otsuka,*† Miho Mizuno,* Chiharu Tomi,* Takashi Yamamura,* and Sachiko Miyake*

From the Department of Immunology, National Institute of Neuroscience, National Center of Neurology and Psychiatry, Tokyo; and the Third Department of Internal Medicine,† Tokyo Medical University, Tokyo, Japan*

Carcinoembryonic antigen-related cellular adhesion molecule 1 (CEACAM1) is a CEA family member that has been reported to have an important role in the regulation of Th1-mediated colitis. In this study, we examined the role of CEACAM1 in an animal model of multiple sclerosis, experimental autoimmune encephalomyelitis (EAE). Treatment of C57BL/6J mice with CEACAM1-Fc fusion protein, a homophilic ligand of CEACAM1, inhibited the severity of EAE and reduced myelin oligodendrocyte glycoprotein-derived peptide (MOG_{35-55})-reactive interferon-γ and interleukin-17 production. In contrast, treatment of these animals with AgB10, an anti-mouse CEACAM1 blocking monoclonal antibody, generated increased severity of EAE in association with increased MOG_{35-55}-specific induction of both interferon-γ and interleukin-17. These results indicated that the signal elicited through CEACAM1 ameliorated EAE disease severity. Furthermore, we found that there was both a rapid and enhanced expression of CEACAM1 on invariant natural killer T cells after activation. The effect of CEACAM1-Fc fusion protein and anti-CEACAM1 mAb on both EAE and MOG_{35-55}-reactive cytokine responses were abolished in invariant natural killer T cell–deficient $J\alpha18^{-/-}$ mice. Taken together, the ligation of CEACAM1 negatively regulates the severity of EAE by reducing MOG_{35-55}-specific induction of both interferon-γ and interleukin-17 via invariant natural killer T cell-dependent mechanisms. *(Am J Pathol 2009, 175:1116–1123; DOI: 10.2353/ajpath.2009.090265)*

Carcinoembryonic antigen-related cellular adhesion molecule 1 (CEACAM1), also known as CD66a, is one of the carcinoembryonic antigen family members and is expressed in epithelial cells, endothelial cells, and hematopoietic cells such as monocytes, dendritic cells, natural killer (NK) cells, B cells, and activated T cells.[1–4] It is involved in intercellular adhesion through homophilic or heterophilic interactions and mediates regulatory functions in cellular growth and differentiation. Several splice variants of CEACAM1 have been detected, that differ with respect to the number of extracellular immunoglobulin-like domains, membrane anchorage, and the length of their cytoplasmic tail.[3] Isoforms of CEACAM1 with a long cytoplasmic tail (CEACAM1-L) contain two immunoreceptor tyrosine-based inhibitory motifs and have been shown to negatively regulate epithelial cell activation and tumor cell growth.[3–5] Recently, the specific function of CEACAM1 as a regulator of T cells has been reported *in vitro* and *in vivo*.[6–12] Mice treated with CEACAM1-Fc fusion protein, a homophilic ligand for CEACAM1 that stimulates the signal from CEACAM1, exhibited an immunosuppressive effect on Th1-mediated colitis *in vivo*, with reduced interferon (IFN)-γ production and T-bet activation.[12] However, the significance of CEACAM1 on other inflammatory autoimmune disease models remains unclear.

Experimental autoimmune encephalomyelitis (EAE) is an inflammatory demyelinating disease induced by sensitization against central nervous system (CNS) components such as myelin oligodendrocyte glycoprotein

Supported by Grant-in-Aid for Scientific Research (B: 7210 to S.M.) from the Japan Society for the Promotion of Science, and the Health and Labour Sciences Research Grants on Research on Psychiatric and Neurological Diseases and Mental Health (to T.Y.) from the Ministry of Health, Labour, and Welfare of Japan.

M.F. and T.O. contributed equally to this work.

Accepted for publication May 21, 2009.

Address reprint requests to Sachiko Miyake, Department of Immunology, National Institute of Neuroscience, NCNP, Kodaira, Tokyo 187-8502, Japan. E-mail: miyake@ncnp.go.jp.

(MOG).[13] Because the neurological signs of paralysis can be monitored continuously, and demyelinating lesions resemble those found in multiple sclerosis, EAE is considered an animal model of the human demyelinating disease multiple sclerosis.[13–16] Numerous studies have reported that EAE is mediated by $CD4^+$ Th1 cells that produce IFN-γ.[13–16] Recently, this idea was questioned because animals deficient in IFN-γ, IFN-γ receptor, or signal transducer and activator of transcription 1 were still found to develop EAE.[17–21] These data led the identification of an interleukin (IL)-23 derived population of Th cells, IL-17-producing Th17 cells, as alternative potent inducers of severe autoimmunity, including EAE.[22–24] However, mice deficient in T-bet and signal transducer and activator of transcription 4, which thus lack Th1 cells, but have large numbers of Th17 cells, are still resistant to EAE.[21,25] Additionally, Th1 and Th17 cells are observed in the CNS at the peak of EAE and diminish after the recovery.[26] It has now been described that Th1 and Th17 cells might cooperate to induce the development of EAE.[27–29] Thus, elucidation of the mechanisms that regulate the production of both Th1 and Th17 cytokines is important in relation to the regulation of EAE.

In this study, we investigated the role of CEACAM1 in EAE either by CEACAM1 ligation with a homophilic ligand for CEACAM1 (CEACAM1-Fc fusion protein), or by blocking with a CEACAM1-specific antibody, AgB10. Here, we demonstrate that signaling through CEACAM1 suppressed MOG-derived peptide (MOG_{35-55})-induced EAE associated with a reduction in MOG_{35-55}-specific T cell production of IFN-γ and IL-17. Moreover, we have identified invariant natural killer T (iNKT) cells as a critical component in CEACAM1-mediated suppression of EAE. iNKT cells are an unique subset of CD1-restricted T cells that express an invariant T cell receptor (TCR) α chain, composed of Vα14-Jβ18 segments in mice and Vα14-Jβ18 segments in humans, and use a restricted set of Vβ genes.[30–31] Due to the ability to produce a wide variety of cytokines, iNKT cells are thought to play regulatory roles in autoimmune diseases.[32] CEACAM1-mediated suppression of EAE was not observed in iNKT cell-deficient $J\alpha18^{-/-}$ mice, and MOG_{35-55}-specific T cell production of IFN-γ and IL-17 was not modified in $J\alpha18^{-/-}$ mice when treated with either CECAM1-Fc fusion protein or AgB10.

Materials and Methods

Animals and Reagents

C57BL/6J (B6) mice were obtained from CLEA Japan Inc. (Tokyo, Japan). $J\alpha18^{-/-}$ mice were kindly provided by Dr. M. Taniguchi (RIKEN, Tokyo, Japan). All animals were maintained in specific pathogen-free conditions in accordance with institutional guidelines of National Institute of Neuroscience, Tokyo, Japan. MOG_{35-55} (amino acid sequence, MEVGWYRSPFSRVVHLYRNGK) was synthesized at Toray Research Center (Tokyo, Japan). Incomplete Freund's adjuvant and heat-killed *mycobacterium tuberculosis* (H37Ra) were obtained from Difco Laboratories (Detroit, Michigan), and pertussis toxin was obtained from List Biological Laboratories (California). The hybridoma producing CEACAM1-specific antibody, AgB10,[33] was kindly provided by Nicole Beauchemin (McGill Cancer Center), and 293 EBNA cells transfected pCEP4-N-CEACAM-Fc, which produce a homophilic ligand of CEACAM1, CEACAM1-Fc fusion protein were kindly provided by Thomas M. Gallagher (Loyola University Medical Center).[34]

Induction and Evaluation of EAE

EAE was induced in mice as described previously.[35] Briefly, mice were immunized subcutaneously with 100 μg of MOG_{35-55} emulsified in incomplete Freund's adjuvant containing 500 μg of *M. tuberculosis*. Directly after the immunization and 48 hours later, mice were injected intraperitoneally with 200 ng of pertussis toxin. Clinical signs of EAE were assessed daily with a 0 to 6 scoring system (0, no signs; 1, partial loss of tail tonicity; 2, completely limp tail and abnormal gait; 3, partial hindlimb paralysis; 4, complete hindlimb paralysis; 5, fore- and hindlimb paralysis or moribund state; 6, dead).

Preparation of Antibody and Fusion Protein

The hybridomas producing AgB10 were cultured in a humidified atmosphere with 5% CO_2 at 37°C in RPMI 1640 supplemented with 10% heat-inactivated fetal calf serum, 2 mmol/L L-glutamine, and 100 U/ml penicillin/streptomycin. The supernatants were collected and AgB10 was affinity-purified using a protein A column according to the manufacturer's instructions (Millipore, MA). 293 EBNA cells transfected pCEP4-*N*-CEACAM1-Fc were cultured in DMEM containing 10% heat-inactivated fetal calf serum, 2 mmol/L L-glutamine, and 100 U/ml penicillin/streptomycin. CEACAM1-Fc fusion protein was affinity-purified using protein G column from the collected supernatants (Amersham Bioscience, NJ).

MOG_{35-55} -Specific T Cell Response and Cytokine Assay

After immunization with MOG_{35-55}, mice were treated intraperitoneally with the indicated compounds, either 250 μg of AgB10 or 250 μg of control rat IgG antibody (Jackson Immuno Research, PA), or either 250 μg of CEACAM1-Fc fusion protein or 250 μg of a chimeric (mouse/human) anti-human CD20 mAb (rituximab) every second day from the day of immunization, day 0, to day 11. The animals were sacrificed at day 11 and inguinal and popliteal lymph nodes (LN) were sampled. Total LN cells were suspended in RPMI 1640 medium containing 2% syngeneic mouse serum, 2 mmol/L L-glutamine, 5×10^{-5} M/L 2-mercaptoethanol, and 100 U/ml penicillin/streptomycin, and were incubated in 96-well plates with 1×10^6 cells/well in the presence of 0, 1, 10, 30, or 100 mg/ml of MOG_{35-55}. Culture supernatant was collected 48 hours after stimulation, and IFN-γ and IL-17 in the

supernatant were determined by enzyme-linked immunosorbent assay (ELISA) using OptEIA kit (BD Bioscience, CA) and IL-17 ELISA kit (R&D systems), respectively.

Histology

Sixteen days after the immunization with MOG_{35-55}, the spinal cords were sampled and stored in 10% formaldehyde. Paraffin-embedded spinal cords were stained with either H&E or luxol fast blue.

Flow Cytometry

Liver mononuclear cells from B6 mice were isolated by Percoll density-gradient centrifugation. 1×10^6 cells/well were stimulated with 1 mg/ml plate-bound anti-CD3 mAb and 2.5 mg/ml Concanavalin A (ConA) in 96-well plates and collected for the use of flow cytometry. Cells were stained with α-galactosylceramide (α-GC) loaded dimeric mouse CD1 days followed by fluorescein isothiocyanate-conjugated AgB10, phycoerythrin-conjugated mAb A85-1, and allophycocyanin-conjugated anti-TCR β-chain. iNKT cells were gated as α-GC loaded CD1 days dimmer and TCRβ double-positive cells, and T cells were gated as TCRβ single-positive cells. Stained cells were analyzed using a FACSCalibur with CellQuest Software (Becton Dickinson, CA).

In Vivo *Injection of α-GC*

B6 mice were treated intraperitoneally with either 500 μg of AgB10 or 500 μg of control rat IgG antibody. Four days after the treatment, 250 μl of blood was collected at 2 or 6 hours after intravenous injection with 0.6 μg α-GC/dimethyl sulfoxide or control dimethyl sulfoxide. Blood samples were centrifuged at 3000 rpm for 30 minutes at 4°C, and serum was collected and IFN-γ and IL-4 were determined using ELISA kit (BD Bioscience, CA).

Statistics

EAE clinical scores for groups of mice are presented as the mean group clinical score ± SEM, and statistical differences were analyzed by the Mann-Whitney U nonparametric ranking test. Data for cytokines were analyzed with the two-way analysis of variance. In appropriate cases, post hoc comparisons were made.

Results

CEACAM1 Has a Role in Ameliorating EAE

To assess the role of CEACAM1 on EAE, we first examined the effect of CEACAM1-Fc fusion protein encoding the extracellular portion of the mCEACAM1-4L. CEACAM1-Fc fusion protein has been demonstrated to homophilically ligate the CEACAM1 molecule, which has been shown to inhibit IFN-γ production.[12] As shown in

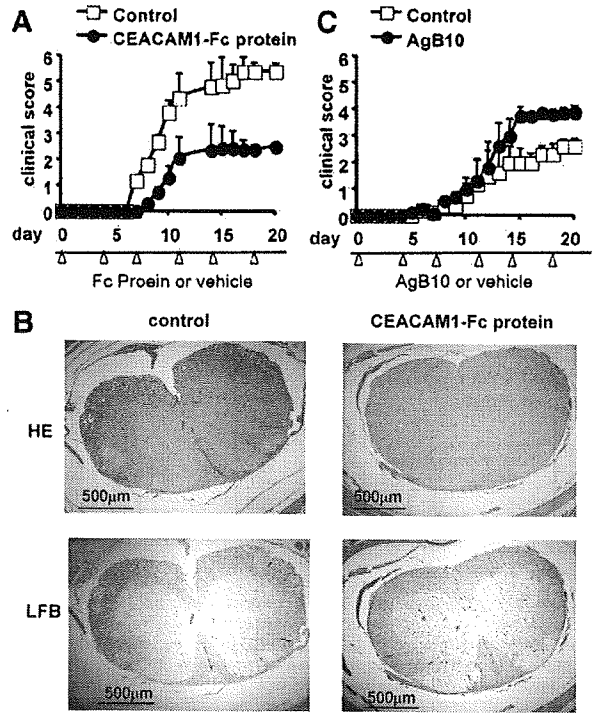

Figure 1. Effect of CEACAM1-Fc fusion protein or CEACAM1-specific antibody on MOG-induced EAE. EAE was induced in B6 mice by immunization with MOG_{35-55}. CEACAM1-Fc fusion protein (**A**) or a mAb for CEACAM1, AgB10 (**C**) was given twice per week starting from the day of immunization. **Arrowheads** indicate the time point of administration of CEACAM1 Fc fusion protein or AgB10. $^*P < 0.05$ vs. Control. The results represent the means ± SEM of eight mice per group. Representative data from two separate experiments is demonstrated. **B:** Histopathological assessment of the CNS region in EAE-induced mice. Shown are cellular infiltration and demyelination of the spinal cord of control or CEACAM1-Fc fusion protein-treated mice on day 16. Paraffin-embedded spinal cords were stained with H&E (**upper** panels) or luxol fast blue (LFB) (**lower** panels). Scale bar = 500 μm.

Figure 1A, administration of CEACAM1-Fc fusion protein significantly inhibited the development and the progression of EAE compared with control mice.

To characterize the immunosuppressive effect of CEACAM1, we performed the pathological analysis of CNS inflammation and demyelination in EAE-induced mice treated with CEACAM1-Fc fusion protein (Figure 1B). Histological examination of the spinal cord 16 days after EAE induction revealed less cellular infiltration and demyelination in CEACAM1-Fc fusion protein-treated mice, as compared with control mice.

We next examined the effects of CEACAM1 specific antibody, AgB10, on the development and progression of MOG_{35-55}-induced EAE in B6 mice (Figure 1C). Ligation of CEACAM1, either homophilically by CEACAM1-Fc fusion protein or heterophilically by microbial components such as the spike glycoprotein of murine hepatitis virus, has been demonstrated to inhibit the proliferation and cytokine production of T cells.[6-12] In contrast, AgB10 has been reported to enhance the T cell proliferation, indicating that AgB10 acts as a blocking antibody. As expected, the clinical scores of EAE were augmented in the mice treated with AgB10 compared with those of control mice.

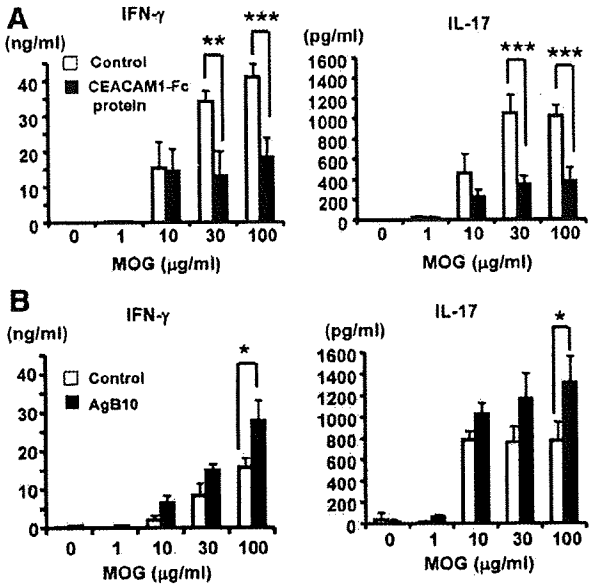

Figure 2. MOG_{35-55}-specific T cell responses in mice treated with CEACAM1-Fc fusion protein or with AgB10. B6 mice were treated with CEACAM1-Fc fusion protein (**A**) or AgB10 (**B**) twice per week from the day of immunization with MOG_{35-55}. Eleven days after the immunization, draining lymph node cells were incubated with MOG_{35-55}. Supernatants were collected from the culture and measured for the concentration of IFN-γ and IL-17 by ELISA. Data represent the mean ± SEM of samples from one of two independent experiments (n = 3 mice). $^*P < 0.05$, $^{**}P < 0.01$, $^{***}P < 0.001$ vs. Control.

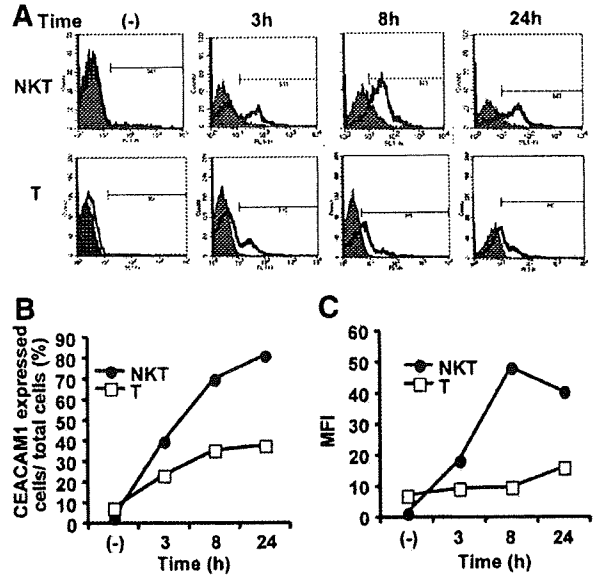

Figure 3. Expression of CEACAM1 on iNKT and T cells, after activation with ConA and anti-CD3 antibody. The histograms show the log fluorescence intensity of CEACAM1 on the surface of iNKT and T cells at the indicated time points after the activation with a combined treatment of ConA and plate bounded anti-CD3 antibody (**A**). The black curves indicate the fluorescence intensity of CEACAM1 on the surface of nontreated cells, and the gray silhouettes show the intensity of activated cells with ConA and anti-CD3 antibody. iNKT cells were gated as α-GC loaded CD1 dimmer and TCRβ double-positive cells, and T cells were gated as TCRβ-positive cells, respectively. The percentage of CEACAM1-expressing cells within total iNKT or T cells and mean fluorescence intensity of the expression at the indicated time points were shown in graph (**B**).

These results indicate that signals through CEACAM1 suppressed both the clinical and the pathological severity of EAE.

The Signal through CEACAM1 Reduces MOG_{35-55}-Specific IFN-γ and IL-17 Production

Since MOG_{35-55} induced EAE is thought to be mediated by MOG_{35-55}-specific Th1 and Th17 cells, we next examined MOG_{35-55}-specific T cell responses in CEACAM1-Fc fusion protein-treated (Figure 2A), or AgB10-treated mice (Figure 2B). We immunized mice with MOG_{35-55} and treated them with either AgB10 or CEACAM1-Fc fusion protein. Twelve days later, we harvested LN cells and re-stimulated them with MOG_{35-55} peptide *in vitro* to examine cytokine production and proliferation. Compared with cells from the control mice, LN cells obtained from CEACAM1-Fc fusion protein treated mice were significantly inhibited in IFN-γ and IL-17 production in responses to MOG_{35-55} re-stimulation (Figure 2A). IL-4 was not detected in the supernatant. On the other hand, *in vivo* treatment with AgB10 showed an enhancement of IFN-γ and IL-17 production in response to MOG_{35-55} stimulation (Figure 2B). Proliferative responses were not significantly different between control mice, CEACAM1-Fc protein-treated, or AgB10-treated mice (data not shown).

These results indicate that the suppressive effect of CEACAM1 on EAE was associated with reduction of MOG_{35-55}-specific IFN-γ and IL-17 production.

Rapid Expression of CEACAM1 on iNKT Cells after Activation

It has been reported that CEACAM1 is expressed on T cells early after activation, and its ligation directly inhibits IFN-γ production by such T cells. We therefore examined the time course of CEACAM1 expression by T cells *in vitro*. As reported previously, CEACAM1 expression was observed on T cells several hours after activation with ConA and anti-CD3 mAb *in vitro*. Moreover, we observed that there was a rapid and higher expression of CEACAM1 by CD1-restricted iNKT cells after activation (Figure 3A). The log fluorescence intensity of CEACAM1 on surface of iNKT and T cells and the percentage of CEACAM1 expressed cells within total iNKT or T cells showed a rapid and also enhanced expression of CEACAM1 on iNKT cells compared with T cells after activation (Figure 3B).

CEACAM1 Regulates IFN-γ Production from iNKT Cells

iNKT cells possess the ability to produce a wide variety of cytokines. Activation of iNKT cells is known to lead to either suppressive or stimulatory immune responses depending on the type of cytokine they produce.[30] We have demonstrated the rapid and enhanced expression of CEACAM1 specifically on iNKT cells (Figure 3A). Thus we next examined whether or not the administration of

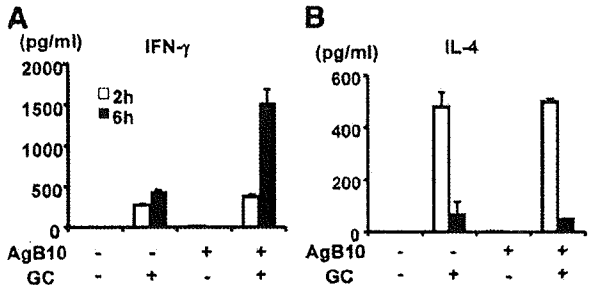

Figure 4. Effect of AgB10 on serum cytokine levels after *in vivo* injection with α-galactosylceramide (α-GC). B6 mice were treated with either AgB10 or control antibody. Four days after the treatment, serum was collected at 2 or 6 hours after intravenous injection of α-GC. Serum levels of IFN-γ and IL-4 were measured by ELISA. Increased levels of IFN-γ were observed in AgB10-α-GC treated mice compared with the control antibody-α-GC treated mice (**A**), whereas no alterations in the level of IL-4 were detected (**B**). Data represent the mean ± SEM of samples from one of three independent experiments (n = 3 mice). ***$P < 0.001$ vs. Control. The results represent the mean concentrations ± SEM of three mice per group.

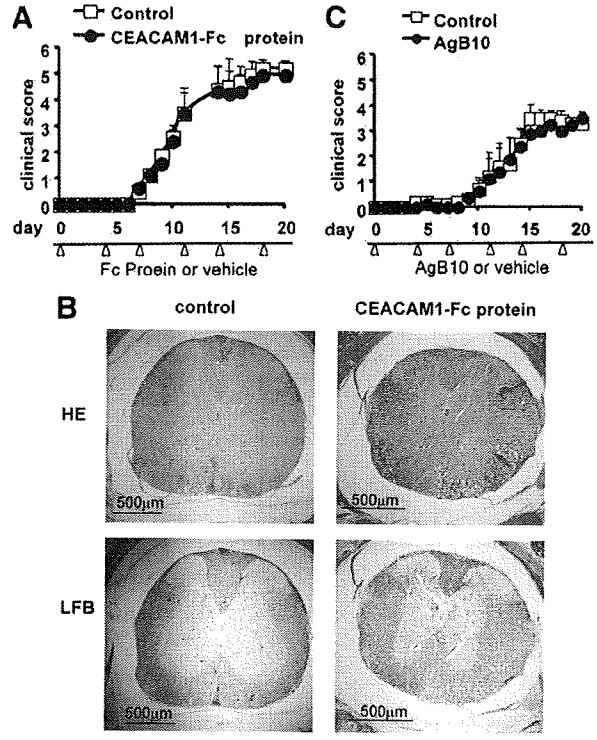

Figure 5. Effect of CEACAM1-Fc fusion protein or CEACAM1-specific antibody on EAE induced in Jα18$^{-/-}$ mice. EAE was induced in *Jα18*$^{-/-}$ mice by immunization with MOG_{35-55}. CEACAM1-Fc fusion protein (**A**) or AgB10 (**C**) was given twice per week starting from the day of immunization. **Arrowheads** indicate the time point of administration of CEACAM1-Fc fusion protein or AgB10. The results represent the means ± SEM of eight mice per group. Representative data from two separate experiments is demonstrated. **B:** Histopathological assessment of the CNS region in *Jα18*$^{-/-}$ mice induced with EAE. Shown are cellular infiltration and demyelination of the spinal cord of control or CEACAM1-Fc fusion protein-treated mice on day 16. Paraffin-embedded spinal cords were stained with H&E (**upper** panel) or LFB (**lower** panels). Scale bar = 500 μm.

AgB10 has an effect on cytokine production by iNKT cells. Mice were injected intravenously with iNKT cell-specific ligand, α-GC, or vehicle, and serum levels of IFN-γ and IL-4 were measured. Mice pretreated with AgB10 and injected with α-GC showed significantly increased level of IFN-γ, as compared with mice treated with control antibody and injected with α-GC (Figure 4A). No significant difference was observed in IL-4 production (Figure 4B). The level of IL-12 in serum was not altered in AgB10-treated mice, and IL-17, IL-21, or IL-23 were not detected in the serum (data not shown). The results suggest that the signal from CEACAM1 have a role in IFN-γ production by iNKT cells.

The Modulation of EAE by CEACAM1 Was Abrogated in iNKT Cell-Deficient Jα18 Mice

Since iNKT cells highly express CEACAM1 after activation, it was of interest to investigate whether the iNKT cells are involved in CEACAM1-mediated amelioration of EAE. To address this question, we examined the effect of CEACAM1-Fc fusion protein on the development of MOG_{35-55}-induced EAE in *Jα18*$^{-/-}$ mice, which genetically lack iNKT cells. In contrast to B6 mice, no alteration in the severity of EAE was observed in CEACAM1-Fc fusion protein treated *Jα18*$^{-/-}$ mice, as compared with control mice (Figure 5A). To further determine the effect of the ligation of CEACAM1 on EAE in *Jα18*$^{-/-}$ mice, we analyzed the CNS inflammation and demyelination in EAE-induced *Jα18*$^{-/-}$ mice treated with CEACAM1-Fc fusion protein. In contrast to wild-type B6 mice, histological examination of the spinal cord of *Jα18*$^{-/-}$ mice showed cellular infiltration and demyelination to a similar extent as sham-treated mice (Figure 5B). We next induced EAE in *Jα18*$^{-/-}$ mice treated with either AgB10 or control antibody. Again, no suppression of clinical EAE was observed in AgB10- treated *Jα18*$^{-/-}$ mice, as compared with the control mice (Figure 5C).

These data show that CEACAM1 signal modulation does not affect on the severity of clinical and pathological EAE in mice lacking iNKT cells.

The Modulation of MOG_{35-55}-Specific IFN-γ and IL-17 Production by CEACAM1 Required iNKT Cells

The suppression of EAE by the ligation of CECAM1 in B6 mice was associated with a reduction in MOG_{35-55}-specific IFN-γ and IL-17 production. We next examined MOG_{35-55}-specific T cell responses in CEACAM1-Fc fusion protein-treated (Figure 6A), or AgB10-treated *Jα18*$^{-/-}$ mice (Figure 6B) by *ex vivo* re-challenge with MOG_{35-55} on day 11 after the immunization of MOG_{35-55}. In contrast to B6 mice, LN cells from CEACAM1-Fc fusion protein-treated *Jα18*$^{-/-}$ mice exhibited no significant reduction of MOG_{35-55} specific IFN-γ and IL-17 production compared with the control mice (Figure 6A). Additionally, *in vivo* treatment of *Jα18*$^{-/-}$ mice with AgB10 also did not significantly enhance of MOG_{35-55}-specific T cell IFN-γ and IL-17 production (Figure 6B).

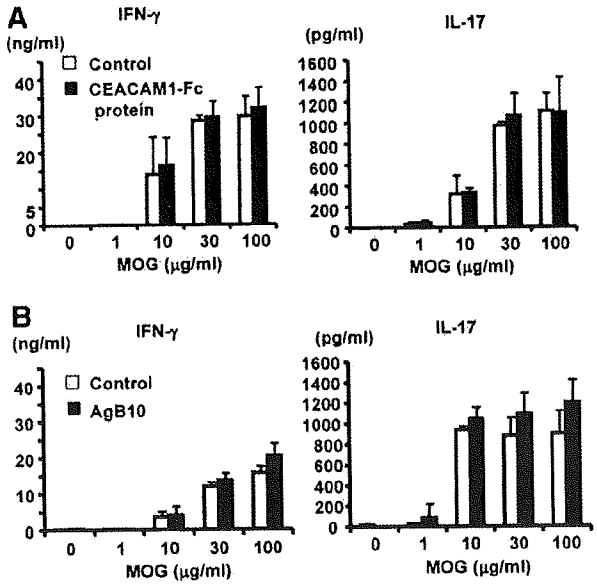

Figure 6. MOG_{35-55}-specific T cell responses in $J\alpha18^{-/-}$ mice treated with CEACAM1-Fc fusion protein or with AgB10. $J\alpha18^{-/-}$ mice were treated with CEACAM1-Fc fusion protein (**A**) or AgB10 (**B**) twice per week from the day of immunization with MOG_{35-55}. Eleven days after the immunization, draining lymph node cells were incubated with MOG_{35-55}. Supernatants were collected from the culture and measured for the concentration of IFN-γ and IL-17 by ELISA. Data represent the mean ± SEM of samples from one of two independent experiments (n = 3 mice).

These results indicate that iNKT cells play an important role in CEACAM1-mediated reduction of MOG-specific IFN-γ and IL-17 production.

Discussion

The present study demonstrated that the signal through CEACAM1 suppressed EAE in association with a reduction in MOG_{35-55}-specific production of IFN-γ and IL-17. Moreover, we showed that CEACAM1 was expressed at an early time point by iNKT cells after activation and CEACAM1 also affected the cytokine production by iNKT cells, including IFN-γ, but not IL-4. Finally, we demonstrated that CEACAM1-mediated modulation of EAE and MOG_{35-55}-specific cytokine production required iNKT cells.

Since both IFN-γ and IL-17 are known as potent inducers of EAE,[21,27–29] CEACAM1-mediated reduction of these cytokines is thought to have a significant role in ameliorating EAE. Although the mechanisms of IFN-γ and IL-17 reduction in CEACAM1-mediated suppression of EAE are not clearly defined so far, we found that the effects of AgB10 and CEACAM1-Fc fusion proteins on EAE and MOG_{35-55}-reactive cytokine responses were abolished in iNKT cell-deficient $J\alpha18^{-/-}$ mice. Thus we concluded that CEACAM1-mediated suppression of EAE was mediated via iNKT cells. Activation of iNKT cells are known to modulate dendritic cell functions, and Kammerer et al reported that AgB10 triggered release of IL-12 from dendritic cells and facilitated priming of naive $CD4^+$ T cells with a Th1-like phenotype.[36] In contrast, Iijima et al showed that CEACAM1-mediated inhibition of Th1-mediated colitis was not dependent on the modulation of IL-12, consistent with this finding, IL-12 was not affected in EAE-induced mice by the *in vivo* treatment of AgB10. Since iNKT cells have been shown to produce IL-21, which promotes the development of Th17 cells,[37] CEACAM1 expression by iNKT cells may have a regulatory role in IL-17 production by Th17 cells via IL-21. However, the production of IL-21 upon iNKT cell activation was not altered by treatment with AgB10. In addition, production of IL-23, which promotes Th17 cell maintenance by activated iNKT cells was not altered in mice treated with AgB10, as compared with control mice. Therefore, the mechanisms how CEACAM1-treated iNKT cells modulate MOG_{35-55} reactive Th1 and Th17 cells remain to be elucidated.

Recently, Mars et al reported that activation of iNKT cells with α-GarCer during priming of the $CD4^+$ T cell response prevents the differentiation of naïve $CD4^+$ T cells toward the Th17 lineage, and the cytokine neutralization experiments indicated that IL-4, IL-10, and IFN-γ are involved in the iNKT cell-mediated regulation of T cell lineage development.[38] Although the direct mechanisms of iNKT cells in regulating the Th17 compartment are still in question, iNKT cells were shown to have a regulatory role in development of the Th17 lineage. Our laboratory reported that antibiotic treatment alters the composition of gut flora, resulting in amelioration of EAE in a iNKT cell-dependent manner.[39] iNKT cell-dependent amelioration of EAE was associated with the suppression of MOG_{35-55}- reactive Th17 cells, although the mechanism by which iNKT cells modulate MOG_{35-55}-reactive Th17 cells remained unclear. It was speculated that altering the compositions of gut flora by antibiotic treatment critically influences the function of iNKT cells, which resulted in a reduction of MOG_{35-55}-reactive Th17 cells. Since various bacterial and viral pathogens *trans*-ligate CEACAM1 and suppresses the activation and proliferation of T cells, it is possible that the alteration of cytokine production in physiological or pathological conditions is partly dependent on the way of *trans*-ligation of pathogens and CEACAM1 on iNKT cells.[3,12,40–45]

In conclusion, this study demonstrates for the first time that CEACAM1 negatively regulates the severity of EAE via an iNKT cell-dependent mechanism. Considering that the selective induction of cytokines by iNKT cells by synthetic ligands has been reported to suppress EAE,[32,46] CEACAM1 may prove to be a novel target for immunotherapy of multiple sclerosis.

Acknowledgments

We thank Masaru Taniguchi at Riken Research Center for Allergy and Immunology (Yokohama, Japan) for providing $J\alpha18^{-/-}$ mice. We thank Thomas M. Gallagher at Loyola University Medical Center (Maywood, IL) for providing 293 EBNA cells transfected with pCEP4-N-CEACAM1-Fc. We thank Nicole Beauchemin (McGill Cancer Center). We are grateful to Ben J.E. Raveney for critical reading of the manuscript.

References

1. Prall F, Nollau P, Neumaier M, Haubeck HD, Drzeniek U, Helmchen U, Loning T, Wagener C: CD66a (BGP), an adhesion molecule of the carcinoembryonic antigen family, is expressed in epithelium, endothelium, and myeloid cells in a wide range of normal human tissues. J Histochem Cytochem 1996, 44:35–41
2. Kammerer R, Hahn S, Singer BB, Luo JS, von Kleist S: Biliary glycoprotein (CD66a), a cell adhesion molecule of the immunoglobulin superfamily, on human lymphocytes: structure, expression and involvement in T cell activation. Eur J Immunol 1998, 28:3664–3674
3. Gray-Owen SD, Blumberg RS: CEACAM1: contact-dependent control of immunity. Nat Rev Immunol 2006, 6:433–446
4. Hammarstrom S: The carcinoembryonic antigen (CEA) family: structures, suggested functions and expression in normal and malignant tissues. Semin Cancer Biol 1999, 9:67–81
5. Izzi L, Turbide C, Houde C, Kunath T, Beauchemin N: Cis-determinants in the cytoplasmic domain of CEACAM1 responsible for its tumour inhibitory function. Oncogene 1999, 18:5563–5572
6. Morales VM, Christ A, Watt SM, Kim HS, Johnson KW, Utku N, Texieira AM, Mizoguchi A, Mizoguchi E, Russell GJ, Russell SE, Bhan AK, Freeman GJ, Blumberg RS: Regulation of human intestinal intraepithelial lymphocyte cytolytic function by biliary glycoprotein (CD66a). J Immunol 1999, 163:1363–1370
7. Nakajima A, Iijima H, Neurath MF, Nagaishi T, Nieuwenhuis EES, Raychowdhury R, Glickman J, Blau DM, Russell S, Holmes KV, Blumberg RS: Activation-induced expression of carcinoembryonic antigen-cell adhesion molecule 1 regulates mouse T lymphocyte function. J Immunol 2002, 168:1028–1035
8. Boulton IC, Gray-Owen SD: Neisserial binding to CEACAM1 arrests the activation and proliferation of CD4$^+$ T lymphocytes. Nat Immunol 2002, 3:229–236
9. Markel G, Wolf D, Hanna J, Gazit R, Goldman-Wohl D, Lavy Y, Yagel S, Mandelboim O: Pivotal role of CEACAM1 protein in the inhibition of activated decidual lymphocyte functions. J Clin Inv 2002, 110:943–953
10. Chen D, Iijima H, Nagaishi T, Nakajima A, Russell S, Raychowdhury R, Morales V, Rudd CE, Utku N, Blumberg RS: Carcinoembryonic antigen-related cellular adhesion molecule 1 isoforms alternatively inhibit and costimulated human T cell function. J Immunol 2004, 172:3535–3543
11. Chen CJ, Shively JE: The cell-cell adhesion molecule carcinoembryonic antigen-related cellular adhesion molecule 1 inhibits IL-2 production and proliferation in human T cells by association with Src homology protein-1 and down-regulates IL-2 receptor. J Immunol 2004, 172:3544–3552
12. Iijima H, Neurath MF, Nagaishi T, Glickman JN, Nieuwenhuis EE, Nakajima A, Chen D, Fuss IJ, Utku N, Lewicki DN, Becker C, Gallagher TM, Holmes KV, Blumberg RS: Specific regulation of T helper cell 1- mediated murine colitis by CEACAM1. J Exp Med 2004, 199:471–482
13. Wekerle H: Experimental autoimmune encephalomyelitis as a model of immune-mediated CNS disease. Curr Opin Neurobiol 1993, 3:779–784
14. Steinman L: Assessment of animal models for MS and demyelinating disease in the design of rational therapy. Neuron 1999, 24:511–514
15. Hemmer B, Archelos JJ, Hartung HP: New concepts in the immunopathogenesis of multiple sclerosis. Nat Rev Neurosci 2002, 3:291–301
16. Sospedra M, Martin R: Immunology of multiple sclerosis. Annu Rev Immunol 2005, 23:683–747
17. Willenborg DO, Fordham S, Bernard CC, Cowden WB, Ramshaw IA: IFN-γ plays a critical down-regulatory role in the induction and effector phase of myelin oligodendrocyte glycoprotein-induced autoimmune encephalomyelitis. J Immunol 1996, 157:3223–3227
18. Krakowski M, Owens T: Interferon-γ confers resistance to experimental allergic encephalomyelitis. Eur J Immunol 1996, 26:1641–1646
19. Willenborg DO, Fordham SA, Staykova MA, Ramshaw IA, Cowden WB: IFN-γ is critical to the control of murine autoimmune encephalomyelitis and regulates both in the periphery and in the target tissue: a possible role for nitric oxide. J Immunol 1999, 163:5278–5286
20. Tran EH, Prince EN, Owens T: IFN-γ shapes immune invasion of the central nervous system via regulation of chemokines. J Immunol 2000, 164:2759–2768
21. Bettelli E, Sullivan B, Szabo SJ, Sobel RA, Glimcher LH, Kuchroo VK: Loss of T-bet, but not STAT1, prevents the development of experimental autoimmune encephalomyelitis. J Exp Med 2004, 200:79–87
22. Cua DJ: Interleukin-23 rather than interleukin-12 is the critical cytokine for autoimmune inflammation of the brain. Nature 2003, 421:744–748
23. Steinman L: A brief history of T(H)17, the first major revision in the T(H)1/T(H)2 hypothesis of T cell mediated tissue damage. Nat Med 2007, 13:139–145
24. Komiyama Y, Nakae S, Matsuki T, Nambu A, Ishigame H, Kakuta S, Sudo K, Iwakura Y: IL-17 plays an important role in the development of experimental autoimmune encephalomyelitis. J Immunol 2006, 177:566–73
25. Chitinis T: Effect of targeted disruption of STAT4 and STAT6 on the induction of experimental autoimmune encephalomyelitis. J Clin Invest 2001, 108:739–747
26. Korn T: Myelin-specific regulatory T-cells accumulate in the central nervous system, but fail to suppress pathogenic effector T-cells at the peak of autoimmune inflammation. Nat Med 2007, 13:423–431
27. Bettelli E, Oukka M, Kuchroo VK: TH-17 cells in the circle of immunity and autoimmunity. Nat Immunol 2007, 8:345–350
28. Stromnes IM, Cerretti LM, Liggitt D, Harris RA, Goverman JM: Differential regulation of central nervous system autoimmunity by Th1 and Th17 cells. Nat Med 2007, 14:337–342
29. Kroenke MA, Carlson TJ, Andjelkovic AV, Segal BM: IL-12- and IL-23-modulated T cells induce distinct types of EAE based on histology. CNS chemokine profile, and response to cytokine inhibition J Exp Med 2008, 205:1535–1541
30. Bendela A, Savage PB, Teyton L. The biology of NKT cells. 2007;25:297–336
31. Kronenberg M: Toward an understanding of NKT cell biology: progress and paradoxes. Annu Rev Immunol 2005, 23:877–900
32. Miyake S, Yamamura T: Therapeutic potential of CD1d-restricted invariant natural killer T cell-based treatment for autoimmune diseases. Int Rev Immunol 2007, 26:73–94
33. Kuprina NI, Baranov VN, Yazova AK, Rudinskaya TD, Escribano M, Cordier J, Gleiverman AS, Goussev AI: The antigen of bile canaliculi of the mouse hepatocyte: identification and ultrastructural localization. Histchemistry 1990, 94:179–186
34. Gallagher TM: A role for naturally occurring variation of the murine coronavirus spike protein in stabilizing association with the cellular receptor. J Virol 1997, 71:3129–3137
35. Miyamoto K, Miyake S, Mizuno M, Oka N, Kusunoki S, Yamamura T: Selective COX-2 inhibitor celecoxib prevents experimental autoimmune encephalomyelitis through COX-2-independent pathway. Brain 2006, 129:1984–1992
36. Kammerer R, Stober D, Singer BB, Obrink B, Reimann J: Carcinoembryonic antigen-related cell adhesion molecule 1 on murine dendritic cells in a potent regulator or T cell stimulation. J Immunol 2001, 166:6537–6544
37. Korn T, Bettelli E, Gao W, Awasthi A, Jager A, Strom TB, Oukka M, Kuchroo VK: IL-21 initiates an alternative pathway to induce proinflammatory T_H17 cells. Nature 2007, 448:484–487
38. Mars LT, Araujo L, Kerschen P, Diem S, Bourgeois E, Van LP, Carrie N, Dy M, Liblau RS, Herbelin A: Invariant NKT cells inhibit development of the Th_{17} lineage. Proc Natl Acad Sci USA 2009, 106: 6238–6243
39. Yokote H, Miyake S, Croxford JL, Oki S, Mizusawa H, Yamamura T: NKT cell-dependent amelioration of a mouse model of multiple sclerosis by altering gut flora. Am J Pathol 2008, 173:1714–1723
40. Gray-Owen SD, Lorenzen DR, Hude A, Meyer TF, Dehio C: Differential Opa specificities for CD66 receptors influence tissue interactions and cellular response to Neisseria Gonorrhoeae. Mol Microbiol 1997, 26:971–980
41. Virji M, Makepeace K, Ferguson DJP, Watt SM: Carcinoembryonic antigens (CD66) on epithelial cells and neutrophils are receptors for Opa proteins of pathogenic neisseriae. Mol Microbiol 1996, 22:941–950
42. Hill DJ, Toleman MA, Evans DJ, Villullas S, Van AL, Virji M: The variable P5 proteins of typeable and non-typeable Haemophilus influenzae target human CEACAM1. Mol Microbiol 2001, 39: 850–862

43. Toleman M, Aho E, Virji M: Expression of pathogen-like Opa adhesions in commensal Neisseria: genetic and functional analysis. Cell Microbiol 2001, 3:33–44
44. Virji M, Evams D, Griffith J, Hill D, Serino L, Hadfield A, Watt SM: Carcinoembryonic antigens are targeted by diverse strains of typable and non-typable Haemophilus influenzae. Mol Microbiol 2000, 36:784–795
45. Berger CN, Billker O, Meyer TF, Servin AL, Kansau I: Differential recognition of members of the carcinoembryonic antigen family by Afa/Dr adhesins of diffusely adhering Escherichia clo (Afa/Dr DAEC). Mol Microbiol 2004, 52:963–983
46. Miyamoto K, Miyake S, Yamamura T: A synthetic glycolipid prevents autoimmune encephalomyelitis by inducing TH2 bias of natural killer T cells. Nature 2001, 413:531–534

Neuropathology and Applied Neurobiology (2009), **35**, 16–35 doi: 10.1111/j.1365-2990.2008.00947.x

Protein microarray analysis identifies human cellular prion protein interactors

J. Satoh*†, S. Obayashi*, T. Misawa*, K. Sumiyoshi*, K. Oosumi* and H. Tabunoki*

**Department of Bioinformatics and Molecular Neuropathology, Meiji Pharmaceutical University, and †Department of Immunology, National Institute of Neuroscience, NCNP, Tokyo, Japan*

J. Satoh, S. Obayashi, T. Misawa, K. Sumiyoshi, K. Oosumi and H. Tabunoki (2009) *Neuropathology and Applied Neurobiology* **35**, 16–35

Protein microarray analysis identifies human cellular prion protein interactors

Aims: To obtain an insight into the function of cellular prion protein (PrPC), we studied PrPC-interacting proteins (PrPIPs) by analysing a protein microarray. **Methods:** We identified 47 novel PrPIPs by probing an array of 5000 human proteins with recombinant human PrPC spanning amino acid residues 23–231 named PR209. **Results:** The great majority of 47 PrPIPs were annotated as proteins involved in the recognition of nucleic acids. Coimmunoprecipitation and cell imaging in a transient expression system validated the interaction of PR209 with neuronal PrPIPs, such as FAM64A, HOXA1, PLK3 and MPG. However, the interaction did not generate proteinase K-resistant proteins. KeyMolnet, a bioinformatics tool for analysing molecular interaction on the curated knowledge database, revealed that the complex molecular network of PrPC and PrPIPs has a significant relationship with AKT, JNK and MAPK signalling pathways. **Conclusions:** Protein microarray is a useful tool for systematic screening and comprehensive profiling of the human PrPC interactome. Because the network of PrPC and interactors involves signalling pathways essential for regulation of cell survival, differentiation, proliferation and apoptosis, these observations suggest a logical hypothesis that dysregulation of the PrPC interactome might induce extensive neurodegeneration in prion diseases.

Keywords: cellular prion protein, KeyMolnet, protein microarray, protein–protein interaction

Published online *Article Accepted* on 23th February 2008

Introduction

Prion diseases are a group of neurodegenerative disorders affecting both animals and humans [1,2]. The great majority of prion diseases are transmissible, and characterized by intracerebral accumulation of an abnormal prion protein (PrPSc) that is identical in amino acid sequence to the cellular isoform (PrPC) encoded by the *PRNP* gene. PrPC is expressed widely in neural and non-neural tissues at the highest level in neurones in the central nervous system (CNS) [3]. PrPSc differs biochemically from PrPC by its β sheet-enriched structure, detergent insolubility, limited proteolysis by proteinase K, a slower turnover rate and infectivity. Previous studies suggested that the protein conformational conversion of α-helix-rich PrPC into β sheet-rich PrPSc involves a homotypic interaction between endogenous PrPC and incoming or *de novo* generated PrPSc via a post-translational process mediated by as yet unidentified species-specific auxiliary factor(s) named 'protein X' [4,5].

At present, the biological function of PrPC remains largely unknown. Several lines of PrPC-deficient mice were established independently by different gene-targeting strategies [6–8]. All of them exhibited normal early development and complete protection against scrapie infection. These observations indicate that PrPC is dispensable for embryonic development, but is pivotal for inducing prion

Correspondence: Jun-ichi Satoh, Department of Bioinformatics and Molecular Neuropathology, Meiji Pharmaceutical University, 2-522-1 Noshio, Kiyose, Tokyo 204–8588, Japan. Tel: +81 42 4958678; Fax: +81 42 4958678; E-mail: satoj@my-pharm.ac.jp

diseases. Several *in vitro* studies suggested a role of PrPC in neuritogenesis [9,10], neuronal cell adhesion [11] and a receptor for neurotrophic factors [12]. More consistently, many studies indicated that an octapeptide repeat region of PrPC with a copper-binding capacity exhibits an antioxidant activity [13]. However, none of previous findings provided an adequate explanation for mild phenotypes of PrPC-deficient mice.

A number of previous studies, by employing mainly the yeast two-hybrid (Y2H) screening system, identified a wide variety of PrPC-interacting proteins (PrPIPs). They include synapsin I [14], glial fibrillary acidic protein [15], amyloid precursor-like protein 1 [16], heat shock protein Hsp60 [17–19], the Hsp cofactor STI-1 [20], the antiapoptotic molecule Bcl-2 [21], signal-transducing adapters such as Grb2 [14], ZAP70 [22] and 14-3-3 [23], neurotrophin receptor interacting MAGE homolog [24], tubulin [25], heterogeneous ribonuclear protein A2/B1 [26], casein kinase 2 [27], plasminogen [28], laminin receptor precursor [29], laminin [9] and vitronection [30]. Most of these molecules play a key role in signal-transducing events essential for neuronal function. However, none of them could serve as the chaperone 'protein X'.

The Y2H system is a powerful approach to identify novel protein–protein interactions. However, Y2H screening requires a lot of time and effort, and is often criticized for detecting the interactions unrelated to the physiological setting, and obtaining high rates of false positive interactors caused by spontaneous activation of reporter genes and self-activating bait proteins [31,32]. Recently, protein microarray technology has been established for rapid, systematic and less expensive screening of thousands of protein–protein interactions in a high-throughput fashion [33,34]. The array includes numerous protein targets of various functional classes immobilized on a single glass slide. The protein microarray has important applications in the areas not only of basic biological research on a whole-proteome scale, but also of drug discovery research of target identification [35,36].

In order to establish a therapeutic intervention targeted on prion propagation, it is essential to clarify the biological function of PrPC and the pathological implication of PrPSc, and equally important to identify all human PrPIPs, some of which potentially serve as a candidate for 'protein X'. The present study was designed to identify a comprehensive profile of the human PrPC interactome by analysing a high-density protein microarray, and to obtain an insight into the PrPC–PrPIPs network.

Materials and methods

Preparation of a V5-tagged PrP probe for microarray analysis

Human embryonic kidney cells HEK293, whose genome was modified for the Flp-In system (Flp-In 293; Invitrogen, Carlsbad, CA), contain a single Flp recombination target (FRT) site targeted for the site-specific recombination, integrated in a transcriptionally active locus of the genome, where it stably expresses the *lacZ*–Zeocin fusion gene driven from the pFRT/*lac*Zeo plasmid under the control of SV40 early promoter. The cells were maintained in Dulbecco's modified Eagle's medium supplemented with 10% foetal bovine serum, 100 U/ml penicillin and 100 μg/ml streptomycin (feeding medium) with inclusion of 100 μg/ml zeocin, as described previously [37].

To prepare the probe for protein microarray analysis, the gene encoding a truncated form of human PrPC spanning amino acid residues 23–231 named PR209 was amplified by polymerase chain reaction (PCR) using PfuTurbo DNA polymerase (Stratagene, La Jolla, CA) and the primer sets listed in Table S1 online. The PCR product was then cloned into a mammalian expression vector pSecTag/FRT/V5-His TOPO (Invitrogen) to produce a fusion protein with a C-terminal V5 tag, a C-terminal polyhistidine (6xHis) tag and an N-terminal Ig κ-chain secretion signal. This vector, together with the Flp recombinase expression vector pOG44 (Invitrogen), was transfected in Flp-In 293 cells by Lipofectamine 2000 reagent (Invitrogen). A stable cell line was established after incubating the transfected cells for 1 month in the feeding medium with inclusion of 100 μg/ml hygromycin B. In this system, the recombinant protein was secreted into the culture medium after the Ig κ-chain secretion signal sequence was processed by an endogenous signal peptidase-mediated cleavage.

To purify the V5-tagged PR209 protein, the serum-free culture supernatant was harvested, and concentrated at a 1/40 volume by centrifugation on an Amicon Ultra-15 filter (Millipore, Bedford, MA). It was then purified by the HIS-select spin column (Sigma, St. Louis, MO), and concentrated at a 1/10 volume by centrifugation on a Centricon-10 filter (Millipore). The protein concentration was determined by a Bradford assay kit (Bio-Rad, Hercules, CA). The purity and specificity of the probe were verified by Western blot analysis using mouse monoclonal anti-V5 antibody (Invitrogen), mouse monoclonal anti-

PrP antibody 3F4 (Dako, Tokyo, Japan) and rabbit polyclonal antibody C20 specific for the sequence close to the C-terminus of PrPC (Santa Cruz Biotechnology, Santa Cruz, CA). To determine the status of glycosylation, 5 μg of the probe protein was deglycosylated by incubating it at 37°C for 1.5 h with 5000 U peptide N-glycosidase F (New England BioLabs, Beverly, MA), followed by separation on the gel [37].

Protein microarray analysis

The present study utilized the ProtoArray human protein microarray v3.0 (Invitrogen). It contains approximately 5000 recombinant GST-tagged human proteins expressed by the baculovirus expression system and purified under native conditions by using gluthathione affinity chromatography to ensure the preservation of native structure, post-translational modifications and proper functionality of target proteins [36,38]. They were spotted in duplicate on a nitrocellulose-coated glass slide. The target proteins cover a wide range of biologically important proteins selected from the human ultimate open reading frame (ORF) clone collection (Invitrogen). The probe is spatially accessible to all parts of target proteins on the array, which protrude from the glass slide surface via the N-terminal GST fusion tag serving as a spacer. The complete list is shown in Table S2 online. The proteins are spotted in an arrangement of 4 × 12 subarrays equally spaced in vertical and horizontal directions. Each subarray includes 20 × 20 spots, composed of 76 positive and negative control spots (C), 222 human target proteins (H), and 102 blanks and empty spots (B) (Figure 1b). The 14 positive control spots include four of an Alexa Fluor 647-labelled antibody (row 1, columns 1, 2; row 14, columns 13, 14), six of a concentration gradient of a biotinylated anti-mouse antibody with a capacity to bind to mouse monoclonal anti-V5 antibody conjugated with Alexa Fluor 647 (row 14, columns 15–20), and four of a concentration gradient of V5 protein (row 15, columns 5–8). The 62 negative control spots include six of a concentration gradient of bovine serum albumin (BSA) (row 1, columns 3–8), four of a concentration gradient of a rabbit anti-GST antibody (row 1, columns 9–12), four of a concentration gradient of calmodulin (row 1, columns 13–16), 16 of a concentration gradient of GST (row 1, columns 17–20; row 2, columns 1–12), 10 of buffer only (row 15, columns 1, 2, 9–16), eight of human IgG subclasses (row 15, columns 17–20; row 16, columns 1–4), 12 of Invitrogen internal controls (row 4, columns 9, 10; row 6, columns 15–18; row 7, columns 9, 10, 15, 16; row 8, columns 13, 14), and two of an antibiotin antibody (row 15, columns 3, 4).

Non-specific binding was blocked by incubating the array for 90 min in the PBST blocking buffer composed of 1% BSA and 0.1% Tween 20 in phosphate-buffered saline (PBS). Then, it was incubated for 30 min at 4°C with the probe described above at a concentration of 200 μg/ml in the probing buffer composed of 1% BSA, 5 mM $MgCl_2$, 0.5 mM dithiothreitol, 0.05% Triton X-100 and 5% glycerol in PBS. The array was washed three times with the probing buffer, and then incubated for 30 min at 4°C with mouse monoclonal anti-V5 antibody labelled with Alexa Fluor 647 (Invitrogen) at a concentration of 260 ng/ml in the probing buffer. Then, the array was washed three times with the probing buffer, and scanned by the GenePix 4200 A scanner (Axon Instruments, Union City, CA) at a wavelength of 635 nm. The data were analysed by using the ProtoArray Prospector software v3.0 (Invitrogen), following acquisition of the microarray lot-specific information, which compensates inter-lot variations in protein concentrations identified by the post-printing quality control. According to the manufacturer-recommended setting of the ProtoArray Prospector software, the spots showing the background-subtracted signal intensity value greater than the median plus three standard deviations of all the fluorescence intensities were considered as having significant interactions. The Z-score, an indicator for statistical significance of binding specificity, was calculated as the background-subtracted signal intensity value of the target protein minus the average of the background-subtracted signal intensity value from the negative control distribution, divided by the standard deviation of the negative control distribution.

Bioinformatics analysis

The gene expression pattern of mouse orthologues of PrPIPs in the brain was searched on the Allen Brain Atlas database [39], an anatomically comprehensive digital atlas containing the expression patterns of more than 20 000 genes in the adult mouse brain analysed by high-throughput *in situ* hybridization methods (http://www.brain-map.org).

The interaction of PrPC with PrPIPs was searched on the Biomolecular Interaction Network database (BIND) (http://bond.unleashedinformatics.com). Functional

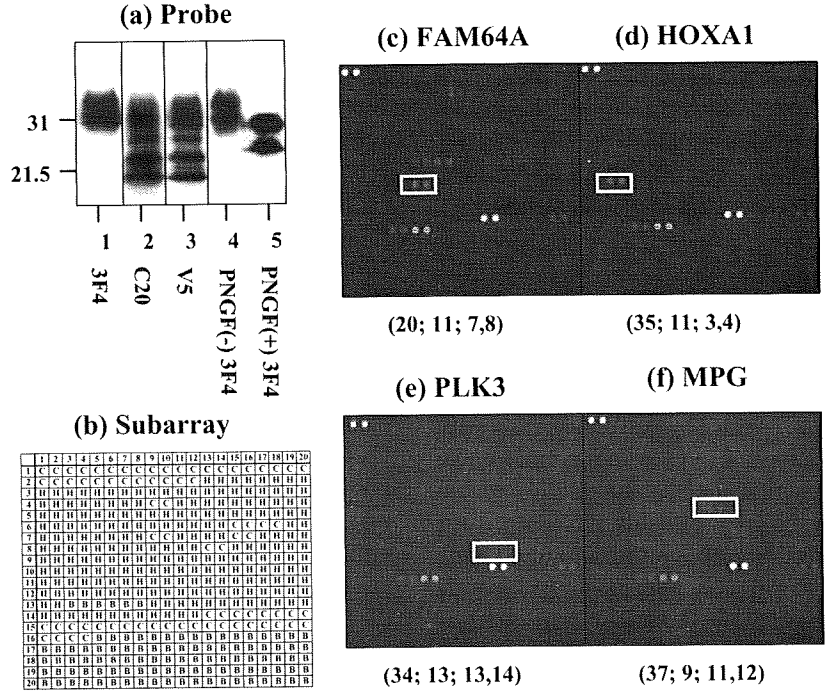

Figure 1. Protein microarray analysis. (a) Western blot of PR209 probe. The lanes (1–5) represent the immunolabelling with the antibodies following: (1) 3F4, (2) C20, (3) V5, (4) 3F4 before treatment with peptide N-glycosidase F (PNGase F) and (5) 3F4 after treatment with PNGase F. (b) The layout of subarray. The high-density protein microarray (5000 proteins, duplicate spots each) utilized in the present study contains 4 × 12 subarrays. Each subarray includes 20 × 20 spots. They are composed of 76 control spots (C) including 14 positive and 62 negative control spots, 222 human target proteins (H) and 102 blanks and empty spots (B), as described in *Materials and methods*. (c) FAM64A. The spot location is subarray 20, row 11, columns 7, 8. (d) HOXA1. Subarray 35, row 11, columns 3, 4. (e) PLK3. Subarray 34, row 13, columns 13, 14. (f) MPG. Subarray 37, row 9, columns 11, 12. PR209 interactors located on different subarrays (c–f) are indicated by an enclosed yellow line. It is worthy to note that in each subarray, positive control spots composed of an Alexa Fluor 647-labelled antibody (row 1, columns 1, 2; row 14, columns 13, 14), a concentration gradient of a biotinylated anti-mouse antibody with a capacity to bind to mouse monoclonal anti-V5 antibody conjugated with Alexa Fluor 647 (row 14, columns 15–20; signals visible on the higher concentration), and a concentration gradient of V5 protein (row 15, columns 5–8; signals visible on the higher concentration) are identified as positive, whereas negative control spots composed of a concentration gradient of BSA (row 1, columns 3–8), a concentration gradient of a rabbit anti-GST antibody (row 1, columns 9–12), a concentration gradient of calmodulin (row 1, columns 13–16), a concentration gradient of GST (row 1, columns 17–20; row 2, columns 1–12), buffer only (row 15; columns 1, 2, 9–16), human IgG subclasses (row 15, columns 17–20; row 16, columns 1–4), Invitrogen internal controls (row 4, columns 9, 10; row 6, columns 15–18; row 7, columns 9, 10, 15, 16; row 8, columns 13, 14), and an antibiotin antibody (row 15, columns 3, 4) are found as negative.

annotation of PrPIPs was searched by the web-accessible program named Database for Annotation, Visualization and Integrated Discovery (DAVID) version 2007, National Institute of Allergy and Infectious Diseases, National Institutes of Health (NIH) (http://david.abcc.ncifcrf.gov) [40]. It covers more than 40 annotation categories, including Gene Ontology terms, protein–protein interactions, protein functional domains, disease associations, biological pathways, sequence general features, homologies, gene functional summaries and tissue expressions. By importing the list of Entrez gene IDs of PrPIPs, this program creates the functional annotation chart, an annotation term-focused view that lists annotation terms and their associated genes under study. To avoid excessive counting of duplicated genes, the Fisher's exact statistics is calculated based on corresponding DAVID gene IDs by which all redundancies in original IDs are removed.

The molecular network of PrPIPs was analysed by the software named KeyMolnet (Institute of Medicinal Molecular Design, Tokyo, Japan) [41]. It operates on a comprehensive knowledge database, composed of information on relationships among human genes, molecules, diseases, pathways and drugs, carefully curated by expert biologists from review articles, literature and public

databases. They are categorized into the core contents collected from selected review articles with the highest reliability or the secondary contents extracted from abstracts of PubMed database and Human Reference Protein database.

By importing the list of Entrez gene IDs, KeyMolnet automatically provides corresponding molecules as a node on networks [41,42]. Among various network-searching algorithms, the 'N-points to N-points' search extracts the molecular network with the shortest route connecting the starting-point molecules and the end-point molecules. The generated network was compared side by side with 346 human canonical pathways of the KeyMolnet library. The algorithm counting the number of overlapping molecular relations between the extracted network and the canonical pathway makes it possible to identify the canonical pathway showing the most significant contribution to the extracted network. The significance in the similarity between both is scored following the formula, where O = the number of overlapping molecular relations between the extracted network and the canonical pathway, V = the number of molecular relations located in the extracted network, C = the number of molecular relations located in the canonical pathway, T = the number of total molecular relations (approximately 90 000 sets) and X = the sigma variable that defines incidental agreements.

$$\text{score} = -\log_2\left(\sum_{x=0}^{Min(C,V)} f(x)\right)$$

$$f(x) = {}_{C}C_{X} \cdot {}_{T-C}C_{V-X} / {}_{T}C_{V}$$

Immunoprecipitation and Western blot analysis

PR209, the N-terminal half of PR209 (amino acid residues 23–121), the C-terminal half of PR209 (amino acid residues 122–231), and the ORF of family with sequence similarity 64, member A (FAM64A), polo-like kinase 3 (PLK3), N-methylpurine-DNA glycosylase (MPG) and homeobox A1 (HOXA1) were amplified by PCR using PfuTurbo DNA polymerase and the primer sets listed in Table S1 online. They were then cloned into the mammalian expression vector p3XFLAG-CMV7.1 (Sigma) or pCMV-Myc (Clontech, Mountain View, CA) to express a fusion protein with an N-terminal Flag or Myc tag. At 48 h after co-transfection of the vectors, HEK293 cells were homogenized in M-PER lysis buffer (Pierce, Rockford, IL) supplemented with a cocktail of protease inhibitors (Sigma). In limited experiments, a proteasome inhibitor MG-132 (Merck-Calbiochem, Tokyo, Japan) was added at a final concentration of 10 μM in the culture medium during the last 24 h before harvest. After preclearance, the supernatant was incubated at 4°C for 3 h with mouse monoclonal anti-Flag M2 affinity gel (Sigma), rabbit polyclonal anti-Myc-conjugated agarose (Sigma) or the same amount of normal mouse or rabbit IgG-conjugated agarose (Santa Cruz Biotechnology). After several washes, the immunoprecipitates were processed for Western blot analysis using rabbit polyclonal anti-Myc antibody (Sigma) and mouse monoclonal anti-FLAG M2 antibody (Sigma). The specific reaction was visualized using a chemiluminescence substrate (Pierce).

To determine the proteinase K-resistant property of PR209, the cells were homogenized in M-PER lysis buffer without inclusion of protease inhibitors. The protein extract was then incubated at 37°C for 30 min with 5 μg/ml recombinant proteinase K (Roche Diagnostics, Mannheim, Germany), followed by adding phenylmethylsulphonyl fluoride at a final concentration of 5 mM, according to the methods described previously [43]. Proteins were precipitated by adding 6% trichloroacetic acid. After centrifugation at 4°C for 15 min at 16 100 g, the pellets were washed with cold acetone, and processed for Western blot analysis using 3F4 antibody.

To determine the detergent-insoluble property of PR209, the cells were homogenized in a lysis buffer containing 100 mM NaCl, 10 mM EDTA, 10 mM Tis (pH 7.4), 0.5% Nonidet P-40 and 0.5% sodium deoxycholate, according to the methods described previously [44]. The lysate was centrifuged at 4°C for 10 min at 2000 g to remove debris. Then, the supernatant was further centrifuged at 4°C for 1 h at 16 100 g to separate detergent-soluble (supernatant) and detergent-insoluble (pellet) fractions. They were processed for Western blot analysis using 3F4 antibody. HRP-conjugated secondary antibodies were obtained from Santa Cruz Biotechnology.

Cell imaging analysis

PR209 and the ORF of FAM64A, PLK3, MPG and HOXA1 were amplified by PCR using PfuTurbo DNA polymerase and the primer sets listed in Table S1 online. They were then cloned into the mammalian expression vector pDsRed-Express-C1 (Clontech), pEYFP-C1 (Clontech), pcDNA3.1/NT/GFP-TOPO (Invitrogen) or pcDNA3.1/CT/GFP-TOPO (Invitrogen) to express a fusion protein with an N-terminal or C-terminal DsRed, EYFP or GFP tag. At 24–48 h after co-transfection of the vectors, the cells were

fixed briefly in 4% paraformaldehyde, mounted on slides with glycerol-polyvinyl alcohol, and examined on the Olympus BX51 universal microscope.

Human neural cell lines and cultures

Human astrocytes (AS) in culture were established from neuronal progenitor (NP) cells of human foetal brain (Cambrex, Walkersville, MD). For the induction of neuronal differentiation, NTera2 cells maintained in the undifferentiated state (NTera2-U) were incubated for 4 weeks in feeding medium containing 10^{-5} M *all trans* retinoic acid (Sigma), replated twice and then plated on a surface coated with Matrigel Basement Membrane Matrix (Becton Dickinson, Bedford, MA). They were incubated for another 2 weeks in feeding medium containing a cocktail of mitotic inhibitors, resulting in the enrichment of differentiated neurones (NTera2-N), as described previously [45]. Human microglia cell line HMO6 was provided by Dr Seung U. Kim, Division of Neurology, University of British Columbia, Vancouver, B.C., Canada. Total RNA of the human frontal cerebral cortex was obtained from Clontech.

Reverse transcription-PCR analysis

DNase-treated total cellular RNA was processed for cDNA synthesis using oligo(dT)$_{12-18}$ primers and SuperScript II reverse transcriptase (Invitrogen). Then, cDNA was amplified by PCR using HotStar Taq DNA polymerase (Qiagen, Valencia, CA) and a panel of primer sets listed in Table S1 online. The amplification program consisted of an initial denaturing step at 95°C for 15 min, followed by a denaturing step at 94°C for 1 min, an annealing step at 60°C for 40 s and an extension step at 72.9°C for 50 s for 30–35 cycles, except for the glyceraldehyde-3-phosphate dehydrogenase (G3PDH), an internal control, amplified for 27 cycles.

Results

Protein microarray analysis identified 47 novel PrPC interactors

To analyse the human protein microarray, V5-tagged PR209 probe was purified from the supernatant of a stable cell line secreting the recombinant protein in the culture medium. By Western blot analysis, the probe was composed of a mixture of glycosylated full-length and N-terminally truncated forms of PrPC (Figure 1a, lanes 1–5). The 18.5-kDa protein identified by C20 but not by 3F4 represents the C-terminal fragment produced by constitutive metalloprotease-mediated cleavage [46]. Among total 5000 proteins on the array, 47 were identified as the proteins showing significant interaction with the probe (Table 1). They include FAM64A (Figure 1c), HOXA1 (Figure 1d), casein kappa (CSN3), bromodomain adjacent to zinc finger domain, 2B (BAZ2B), chromosome 7 ORF 50 (C7orf50), surfeit 2 (SURF2), sodium channel modifier 1 (SCNM1), chromosome 18 ORF 56 (C18orf56), PLK3 (Figure 1e), RNA binding motif protein 22 (RBM22), hypothetical protein DKFZp761B107, MPG (Figure 1f), zinc finger protein 192 (ZNF192), thymic stromal lymphopoietin (TSLP), DEAD box polypeptide 47 (DDX47), MAP/microtubule affinity-regulating kinase 4 (MARK4), zinc finger protein 408 (ZNF408), TBP-like 1 (TBPL1), activator of basal transcription 1 (ABT1), ribosomal protein L41 (RPL41), zinc finger protein 740 (ZNF740), CWC15 homolog, four and a half LIM domains 1 (FHL1), amyotrophic lateral sclerosis 2 chromosome region, candidate 4 (ALS2CR4), immediate early response 3 (IER3), KIAA1191, peptidyl-tRNA hydrolase 1 homolog (PTRH1), phosphodiesterase 4D interacting protein (PDE4DIP), Rho GTPase activating protein 15 (ARHGAP15), mitochondrial GTPase 1 homolog (MTG1), cirrhosis, autosomal recessive 1 A (CIRH1A), eukaryotic translation initiation factor 2C, 1 (EIF2C1), WD repeat domain 5 (WDR5), centaurin, alpha 2 (CENTA2), protein phosphatase 1, regulatory subunit 14 A (PP1R14 A), cold inducible RNA binding protein (CIRBP), zinc finger, FYVE domain containing 28 (ZFYVE28), within bgcn homolog (WIBG), nucleolar protein family A, member 2 (NOLA2), PTPRF interacting protein, binding protein 2 (PPFIBP2), family with sequence similarity 27, member E3 (FAM27E3), fibroblast growth factor 13 (FGF13), apoptosis-inducing factor, mitochondrion-associated, 3 (AIFM3), 2′,3′-cyclic nucleotide 3′ phosphodiesterase (CNP), NIN1/RPN12 binding protein 1 homolog (NOB1), RNA-binding region containing 3 (RNPC3) and dual-specificity tyrosine-phosphorylation regulated kinase 3 (DYRK3). The gene expression pattern of PrPC interactors (PrPIPs) in the adult brain analysed by *in situ* hybridization was searched on the Allen Brain Atlas database [39]. Among 47 PrPIPs, at least 35 mouse orthologues (74%) were expressed in various regions of the adult mouse brain (Table 1). The expression pattern of the remaining

Table 1. PrPC-interacting proteins (PrPIPs) identified by protein microarray analysis

No.	Entrez gene ID	Gene symbol	Gene name	Putative molecular function	Block	Row	Column	Z-score	Gene expression in adult mouse brain (region with the highest expression level)
1	54478	FAM64A	Family with sequence similarity 64, member A	A protein with the DUF1466 domain of unknown function	20	11	7, 8	21.89656	Unknown
2	3198	HOXA1	Homeobox A1	A transcription factor that regulates the placement of hindbrain segments in the proper location along the anterior–posterior axis during development	35	11	3, 4	18.36074	Yes (CB)
3	1448	CSN3	Casein kappa	A milk protein	20	9	9, 10	12.58106	Yes (OLF)
4	29994	BAZ2B	Bromodomain adjacent to zinc finger domain, 2B	A component of chromatin remodeling complexes	24	10	5, 6	7.96988	Yes (MY)
5	84310	C7orf50	Chromosome 7 open reading frame 50	A hypothetical protein of unknown function	21	11	9, 10	6.7938	Unknown
6	6835	SURF2	Surfeit 2	The housekeeping gene of unknown function	15	9	15, 16	6.31368	Yes (MY)
7	79005	SCNM1	Sodium channel modifier 1	A zinc finger protein acting as a premRNA splicing factor	18	6	3, 4	6.06453	Yes (CB and other regions)
8	494514	C18orf56	Chromosome 18 open reading frame 56	A hypothetical protein of unknown function	10	10	19, 20	6.02515	Unknown
9	1263	PLK3	Polo-like kinase 3 (Drosophila)	A serine/threonine kinase that regulates cell cycle progression	34	13	13, 14	5.94109	Yes (MY)
10	55696	RBM22	RNA binding motif protein 22	A zinc finger protein with the RNA recognition motif of unknown function	20	9	7, 8	5.67225	Yes (CB)
11	91050	DKFZp761B107	Hypothetical protein DKFZp761B107	A protein with the SMC N-terminal domain of unknown function	22	12	3, 4	5.36251	Unknown
12	4350	MPG	N-methylpurine-DNA glycosylase	A DNA glycosylase acting as a DNA repair enzyme	37	9	11, 12	5.16637	Yes (RHP)
13	7745	ZNF192	Zinc finger protein 192	A Kruppel family zinc finger transcription factor	21	11	13, 14	5.12927	Unknown
14	85480	TSLP	Thymic stromal lymphopoietin	A haemopoietic cytokine that enhances the maturation of dendritic cells	21	10	19, 20	4.92555	Yes (RHP)
15	51202	DDX47	DEAD (Asp-Glu-Ala-Asp) box polypeptide 47	A member of the DEAD box protein family RNA helicases	2	11	11, 12	4.90132	Yes (MY)
16	57787	MARK4	MAP/microtubule affinity-regulating kinase 4	A serine/threonine kinase that regulates microtubule organization in neuronal cells	12	13	5, 6	4.38333	Yes (TH)
17	79797	ZNF408	Zinc finger protein 408	A zinc finger protein with the SFP1 domain acting as a transcriptional repressor that regulates cell cycle	21	11	19, 20	4.27504	Unknown

 Neuropathology and Applied Neurobiology, **35**, 16–35

18	9519	TBPL1	TBP-like 1	A general transcription factor that regulates spermatogenesis	3	12	1, 2	4.16447	Yes (OLF)
19	29777	ABT1	Activator of basal transcription 1	A basal transcriptional activator	36	9	15, 16	3.97136	Yes (OLF)
20	6171	RPL41	Ribosomal protein L41	A componet of the 60S ribosome subunit	14	10	7, 8	3.9388	Unknown
21	283337	ZNF740	Zinc finger protein 740	A zinc finger protein of unknown function	20	9	15, 16	3.88503	Unknown
22	51503	CWC15	CWC15 homolog (S. cerevisiae)	A cell cycle control protein involved in mRNA splicing	19	7	13, 14	3.78582	Unknown
23	2273	FHL1	Four and a half LIM domain 1	A protein with the LIM domain that regulates skeletal muscle differentiation	26	3	11, 12	3.75175	Yes (sAMY)
24	65062	ALS2CR4	Amyotrophic lateral sclerosis 2 (juvenile) chromosome region, candidate 4	A membrane protein of unknown function	34	7	7, 8	3.69722	Yes (RHP)
25	8870	IER3	Immediate early response 3	The immediate early gene acting as an antiapoptosis regulator	26	10	13, 14	3.6018	Yes (CB)
26	57179	KIAA1191	KIAA1191	A cytoplasmic protein of unknown function	10	10	13, 14	3.56924	Unknown
27	138428	PTRH1	Peptidyl-tRNA hydrolase 1 homolog (S. cerevisiae)	A peptidyl-tRNA hydrolase	47	10	19, 20	3.55258	Yes (CTX)
28	9659	PDE4DIP	Phosphodiesterase 4D interacting protein (myomegalin)	A protein of the golgi/centrosome that interacts with a cyclic nucleotide phosphodiesterase	25	11	1, 2	3.54046	Yes (HIP)
29	55843	ARHGAP15	Rho GTPase activating protein 15	A Rho GTPase-activating protein acting as a regulator of RAC1	9	6	13, 14	3.50411	Yes (CTX)
30	92170	MTG1	Mitochondrial GTPase 1 homolog (S. cerevisiae)	A mitochondrial GTPase	48	14	7, 8	3.49729	Yes (HIP)
31	84916	CIRH1A	Cirrhosis, autosomal recessive 1 A (cirhin)	A mitochondrial protein with WD40 repeats of unknown function	14	10	19, 20	3.4511	Yes (HIP)
32	26523	EIF2C1	Eukaryotic translation initiation factor 2C, 1	A member of the Argonaute family (AGO1) that plays a role in siRNA-mediated gene silencing	18	11	11, 12	3.43671	Yes (HIP)
33	11091	WDR5	WD repeat domain 5	A protein with WD40 repeats that constitutes a component of histone methyltransferase complexes	20	7	9, 10	3.37083	Yes (HIP)
34	55803	CENTA2	Centaurin, alpha 2	A plasma membrane GTPase activating protein with PH domains	47	12	5, 6	3.25269	Yes (MY)
35	94274	PPP1R14 A	Protein phosphatase 1, regulatory (inhibitor) subunit 14 A	A phosphorylation-dependent inhibitor of smooth muscle myosin phosphatase	9	5	3, 4	3.25117	Yes (MY)
36	1153	CIRBP	Cold-inducible RNA binding protein	A cold stress-inducible protein wuth the RNA recognition motif that plays a role in cold-induced suppression of cell proliferation	16	10	3, 4	3.22391	Yes (CTX)